in this area. It is, however, possible to attribute the emergence and spread of the triple and quadruple *dhfr* mutants to the widespread use of SP in Southeast Asia during the 1970s and 1980s.

We consider that weak and persistent pyrimethamine pressure by medicated salt projects, a form of mass drug administration, may explain the first selection of pyrimethamine-resistant parasites (15, 25). In the late 1950s and early 1960s, medicated salt projects were carried out in four different endemic regions: Indonesian Papua, the Thailand-Cambodia border, Ghana, and Iran (15, 25). In Southeast Asia and Melanesia, this project was carried out from 1959 to 1962 and from 1960 to 1961, respectively. Pyrimethamine resistance in *P. falciparum* was reported within 3 months of the start of the project (1960) in Indonesian Papua (7). At the Thailand-Cambodia border, resistance also developed quickly and pyrimethamine was replaced by chloroquine beginning in 1961. A large number of people treated with subcurative doses of antimalarial drugs present ideal conditions for the emergence of drug resistance (4, 27, 28). This, combined with the long half-life of pyrimethamine (116 h) (29), would have facilitated the emergence of drug resistance within the areas covered by the medicated salt project: Indonesian Papua and the Thailand-Cambodia border.

The *dhfr* double mutant (CN<u>RN</u>I), which confers moderate resistance to pyrimethamine, is widely distributed in Africa, West Asia, and Melanesia. However, whether this mutant is regularly selected de novo or whether it has spread from a limited number of foci of emergence is not known. In the present study, only two distinct microsatellite haplotypes (SEA and Melanesia haplotypes) were observed in a total of 184 *P. falciparum* isolates harboring the *dhfr* double mutant from Papua New Guinea, Vanuatu, and the Solomon Islands, suggesting that the generation of two mutations at positions 59 and 108 in *dhfr* is not frequent. In laboratory isolates, key point mutations in *dhfr* have occurred at frequencies as high as 2.5 × 10^{-9} per parasite replication, which predicts the generation of one mutant parasite in every malaria patient, assuming the number of parasites to be 10^{10} to 10^{12} in every infection (14). Consistently, the expected heterozygosities at microsatellite markers around *dhfr* were comparable between the wild-type and single *dhfr* mutant parasites. Thus, the initial mutation at position 108 in *dhfr* may occur relatively frequently (12, 20), but the generation and selection of an additional mutation at position 59 appear to be considerably less frequent. Mutations that render pathogens resistant to drug treatment are often associated with a loss of fitness (8, 11, 26). Resistant mutants may themselves develop compensatory mutations, which could then allow them to grow and survive in competition with wild-type forms (5, 26). The discrepancy between the frequent generation of the mutation at position 108 in *dhfr* and the rare occurrence of the *dhfr* double mutant as observed in this study may thus be reconciled by the requirement of complex compensatory mutations in a locus other than *dhfr* for restoring parasite fitness in natural populations.

In the present study, our samples of Papua New Guinea and Thailand were from individuals with clinical malaria, while samples from other sites were from cross-sectional studies of asymptomatic individuals. Symptomatic patients usually have higher parasite densities than do asymptomatic individuals. Thus, we cannot exclude the possibility that prevalences of

microsatellite haplotypes may differ between isolates that cause disease and those that do not produce symptoms. However, we do not consider it very likely because there was no significant difference in the frequency distribution of genotypes of an antigen gene (*mspl*) between clinical patients and asymptomatic individuals in Melanesia (23).

In conclusion, this study provides strong evidence for the unique and independent origin of pyrimethamine resistance in Melanesia. The *dhfr* mutant, perhaps emerging from West Papua, has the same double mutations found in other geographic areas but distinct microsatellite haplotypes flanking the gene. Our results also show that the generation of double mutants with mutations at positions 59 and 108 of *dhfr* is a rare event, and this double mutation may be a first rate-determining step for the stable persistence of pyrimethamine resistance in *P. falciparum*.

ACKNOWLEDGMENTS

REFERENCES

1. **Bwijo, B., A. Kaneko, M. Takechi, I. L. Zungu, Y. Moriyama, J. K. Lum, T. Tsukahara, T. Mita, N. Takahashi, Y. Bergqvist, A. Bjorkman, and T. Kobayakawa.** 2003. High prevalence of quintuple mutant *dhps/dhfr* genes in *Plasmodium falciparum* infections seven years after introduction of sulfadoxine and pyrimethamine as first line treatment in Malawi. Acta Trop. **85:**363–373.
2. **Cortese, J. F., A. Caraballo, C. E. Contreras, and C. V. Plowe.** 2002. Origin and dissemination of *Plasmodium falciparum* drug-resistance mutations in South America. J. Infect. Dis. **186:**999–1006.
3. **Cowman, A. F., M. J. Morry, B. A. Biggs, G. A. Cross, and S. J. Foote.** 1988. Amino acid changes linked to pyrimethamine resistance in the dihydrofolate reductase-thymidylate synthase gene of *Plasmodium falciparum*. Proc. Natl. Acad. Sci. USA **85:**9109–9113.
4. **Diourté, Y., A. Djimde, O. K. Doumbo, I. Sagara, Y. Coulibaly, A. Dicko, M. Diallo, M. Diakite, J. F. Cortese, and C. V. Plowe.** 1999. Pyrimethamine-sulfadoxine efficacy and selection for mutations in *Plasmodium falciparum* dihydrofolate reductase and dihydropteroate synthase in Mali. Am. J. Trop. Med. Hyg. **60:**475–478.
5. **Levin, B. R., V. Perrot, and N. Walker.** 2000. Compensatory mutations, antibiotic resistance and the population genetics of adaptive evolution in bacteria. Genetics **154:**985–997.
6. **McCollum, A. M., A. C. Poe, M. Hamel, C. Huber, Z. Zhou, Y. P. Shi, P. Ouma, J. Vulule, P. Bloland, L. Slutsker, J. W. Barnwell, V. Udhayakumar, and A. A. Escalante.** 2006. Antifolate resistance in *Plasmodium falciparum*: multiple origins and identification of novel *dhfr* alleles. J. Infect. Dis. **194:** 189–197.
7. **Meuwissen, J. H.** 1961. Resistance of *Plasmodium falciparum* to pyrimethamine and proguanil in Netherlands New Guinea. Am. J. Trop. Med. Hyg. **10:**135–139.
8. **Mita, T., A. Kaneko, J. K. Lum, I. L. Zungu, T. Tsukahara, H. Eto, T. Kobayakawa, A. Bjorkman, and K. Tanabe.** 2004. Expansion of wild type allele rather than back mutation in *pfcrt* explains the recent recovery of chloroquine sensitivity of *Plasmodium falciparum* in Malawi. Mol. Biochem. Parasitol. **135:**159–163.
9. **Mita, T., A. Kaneko, F. Hombhanje, I. Hwaihwanje, N. Takahashi, H.**

Osawa, T. Tsukahara, A. Masta, J. K. Lum, T. Kobayakawa, T. Ishizaki, and A. Bjorkman. 2006. Role of *pfmdr1* mutations on chloroquine resistance in *Plasmodium falciparum* isolates with *pfcrt* K76T from Papua New Guinea. Acta Trop. **98:**137–144.

10. Mita, T., A. Kaneko, I. Hwaihwanje, T. Tsukahara, N. Takahashi, H. Osawa, K. Tanabe, T. Kobayakawa, and A. Bjorkman. 2006. Rapid selection of *dhfr* mutant allele in *Plasmodium falciparum* isolates after the introduction of sulfadoxine/pyrimethamine in combination with 4-aminoquinolines in Papua New Guinea. Infect. Genet. Evol. **6:**447–452.

11. Mita, T., A. Kaneko, J. K. Lum, B. Bwijo, M. Takechi, I. L. Zungu, T. Tsukahara, K. Tanabe, T. Kobayakawa, and A. Bjorkman. 2003. Recovery of chloroquine sensitivity and low prevalence of the *Plasmodium falciparum* chloroquine resistance transporter gene mutation K76T following the discontinuance of chloroquine use in Malawi. Am. J. Trop. Med. Hyg. **68:**413–415.

12. Nair, S., J. T. Williams, A. Brockman, L. Paiphun, M. Mayxay, P. N. Newton, J. P. Guthmann, F. M. Smithuis, T. T. Hien, N. J. White, F. Nosten, and T. J. Anderson. 2003. A selective sweep driven by pyrimethamine treatment in Southeast Asian malaria parasites. Mol. Biol. Evol. **20:**1526–1536.

13. Nei, M. 1987. Molecular evolutionary genetics. Columbia University Press, New York, NY.

14. Paget-McNicol, S., and A. Saul. 2001. Mutation rates in the dihydrofolate reductase gene of *Plasmodium falciparum*. Parasitology **122:**497–505.

15. Payne, D. 1988. Did medicated salt hasten the spread of chloroquine resistance in *Plasmodium falciparum*? Parasitol. Today **4:**112–115.

16. Pearce, R., A. Malisa, S. P. Kachur, K. Barnes, B. Sharp, and C. Roper. 2005. Reduced variation around drug-resistant *dhfr* alleles in African *Plasmodium falciparum*. Mol. Biol. Evol. **22:**1834–1844.

17. Peterson, D. S., W. K. Milhous, and T. E. Wellems. 1990. Molecular basis of differential resistance to cycloguanil and pyrimethamine in *Plasmodium falciparum* malaria. Proc. Natl. Acad. Sci. USA **87:**3018–3022.

18. Plowe, C. V., J. F. Cortese, A. Djimde, O. C. Nwanyanwu, W. M. Watkins, P. A. Winstanley, J. G. Estrada-Franco, R. E. Mollinedo, J. C. Avila, J. L. Cespedes, D. Carter, and O. K. Doumbo. 1997. Mutations in *Plasmodium falciparum* dihydrofolate reductase and dihydropteroate synthase and epidemiologic patterns of pyrimethamine-sulfadoxine use and resistance. J. Infect. Dis. **176:**1590–1596.

19. Reeder, J. C., K. H. Rieckmann, B. Genton, K. Lorry, B. Wines, and A. F. Cowman. 1996. Point mutations in the dihydrofolate reductase and dihydropteroate synthetase genes and in vitro susceptibility to pyrimethamine and cycloguanil of *Plasmodium falciparum* isolates from Papua New Guinea. Am. J. Trop. Med. Hyg. **55:**209–213.

20. Roper, C., R. Pearce, B. Bredenkamp, J. Gumede, C. Drakeley, F. Mosha, D. Chandramohan, and B. Sharp. 2003. Antifolate antimalarial resistance in southeast Africa: a population-based analysis. Lancet **361:**1174–1181.

21. Roper, C., R. Pearce, S. Nair, B. Sharp, F. Nosten, and T. Anderson. 2004. Intercontinental spread of pyrimethamine-resistant malaria. Science **305:** 1124.

22. Sakihama, N., T. Mitamura, A. Kaneko, T. Horii, and K. Tanabe. 2001. Long PCR amplification of *Plasmodium falciparum* DNA extracted from filter paper blots. Exp. Parasitol. **97:**50–54.

23. Sakihama, N., H. Ohmae, B. Bakote'e, M. Kawabata, K. Hirayama, and K. Tanabe. 2006. Limited allelic diversity of *Plasmodium falciparum* merozoite surface protein 1 gene from populations in the Solomon Islands. Am. J. Trop. Med. Hyg. **74:**31–40.

24. Sirawaraporn, W., T. Sathitkul, R. Sirawaraporn, Y. Yuthavong, and D. V. Santi. 1997. Antifolate-resistant mutants of *Plasmodium falciparum* dihydrofolate reductase. Proc. Natl. Acad. Sci. USA **94:**1124–1129.

25. Verdrager, J. 1986. Epidemiology of emergence and spread of drug-resistant falciparum malaria in Southeast Asia. Southeast Asian J. Trop. Med. Public Health **17:**111–118.

26. Walliker, D., P. Hunt, and H. Babiker. 2005. Fitness of drug-resistant malaria parasites. Acta Trop. **94:**251–259.

27. Wang, P., C. S. Lee, R. Bayoumi, A. Djimde, O. Doumbo, G. Swedberg, L. D. Dao, H. Mshinda, M. Tanner, W. M. Watkins, P. F. Sims, and J. E. Hyde. 1997. Resistance to antifolates in *Plasmodium falciparum* monitored by sequence analysis of dihydropteroate synthetase and dihydrofolate reductase alleles in a large number of field samples of diverse origins. Mol. Biochem. Parasitol. **89:**161–177.

28. Watkins, W. M., E. K. Mberu, P. A. Winstanley, and C. V. Plowe. 1997. The efficacy of antifolate antimalarial combinations in Africa: a predictive model based on pharmacodynamic and pharmacokinetic analyses. Parasitol. Today **13:**459–464.

29. Winstanley, P., W. Watkins, D. Muhia, S. Szwandt, E. Amukoye, and K. Marsh. 1997. Chlorproguanil/dapsone for uncomplicated *Plasmodium falciparum* malaria in young children: pharmacokinetics and therapeutic range. Trans. R. Soc. Trop. Med. Hyg. **91:**322–327.

30. Wongsrichanalai, C., A. L. Pickard, W. H. Wernsdorfer, and S. R. Meshnick. 2002. Epidemiology of drug-resistant malaria. Lancet Infect. Dis. **2:**209–218.

31. Wootton, J. C., X. Feng, M. T. Ferdig, R. A. Cooper, J. Mu, D. I. Baruch, A. J. Magill, and X. Z. Su. 2002. Genetic diversity and chloroquine selective sweeps in *Plasmodium falciparum*. Nature **418:**320–323.

Decursin and Decursinol Angelate Selectively Inhibit NADH-Fumarate Reductase of *Ascaris suum*

Kazuro Shiomi[1,2], Hiroko Hatano[2], Hiromi Morimoto[3], Hideaki Ui[1], Kimitoshi Sakamoto[4], Kiyoshi Kita[4], Hiroshi Tomoda[3], Eun Woo Lee[5], Tae Ryeon Heo[6], Hirokazu Kawagishi[7], Satoshi Ōmura[1,2]

Abstract

NADH-fumarate reductase (NFRD) is a key enzyme in many anaerobic helminths. Decursin and decursinol angelate have been isolated from the roots of *Angelica gigas* Nakai (Apiaceae) as NFRD inhibitors. They inhibited *Ascaris suum* NFRD with IC_{50} values of 1.1 and 2.7 μM, respectively. Their target is the electron transport enzyme complex I. Since the inhibitory activities of decursin against bovine heart complexes are weak, it is a selective inhibitor of the nematode complex I. In contrast, decursinol angelate moderately inhibits bovine heart complexes II and III. Decursinol inhibits *A. suum* NFRD to a similar extent, but its target is complex II. It also inhibits bovine heart complexes II and III.

In the course of screening for anthelmintic antibiotics, we have been interested in the differences in energy metabolisms between the host and helminths [1]. The NADH-fumarate reductase (NFRD) system is part of a special respiratory system in parasitic helminths, which is found in many anaerobic organisms. The system is composed of complex I (NADH-rhodoquinone oxidoreductase) and complex II (rhodoquinol-fumarate reductase). Electrons from NADH are accepted by rhodoquinone through complex I, and then transferred to fumarate through complex II. We have screened fungal metabolites for inhibitors of NFRD using *Ascaris suum* (roundworm) mitochondria, and obtained nafuredin and atpenins. Nafuredin is a selective inhibitor of helminth complex I and showed anthelmintic activity *in vivo* [2], [3], [4]. Atpenins are non-selective complex II inhibitors, but they are the most potent complex II inhibitors ever reported [5]. Atpenin A5 is bound to a ubiquinone binding site of complex II, which was revealed by the co-crystal structure of atpenin A5 and the *E. coli* enzyme [6].

Affiliation: [1] Kitasato Institute for Life Sciences, Kitasato University, Tokyo, Japan · [2] The Kitasato Institute, Tokyo, Japan · [3] School of Pharmacy, Kitasato University, Tokyo Japan · [4] Graduate School of Medicine, The University of Tokyo, Tokyo, Japan · [5] PNE Co. Ltd., 907–12 Daechidong, Kangnam-Gu, Seoul, Korea · [6] Faculty of Biological Engineering, Inha University, Incheon, Korea · [7] Graduate School of Science and Technology, Shizuoka University, Shizuoka, Japan

Correspondence: Prof. Kazuro Shiomi · Kitasato Institute for Life Sciences · Kitasato University · 5-9-1 Shirokane · Minato-ku · Tokyo 108-8641 · Japan · Phone: +81-3-5791-6439 · Fax: +81-3-5791-6131 · E-mail: shiomi@lisci.kitasato-u.ac.jp
Prof. Satoshi Ōmura · The Kitasato Institute · 5-9-1 Shirokane · Minato-ku · Tokyo 108-8642 · Japan · Phone: +81-3-5791-6101 · Fax: +81-3-3444-8360 · E-mail: omura-s@kitasato.or.jp

The screening for NFRD inhibitors from herbal medicines led to the isolation of two compounds, decursin (1) [7], [8] and decursinol angelate (2) [9], [10] (Fig. 1), from the roots of *Angelica gigas* Nakai, which have been used for the treatment of anemia and as analgesic, sedative, and tonic agents. Some biological and biochemical activities of 1 and 2 have been reported, such as antibacterial activity against *Helicobacter pylori* [11], antitumor activity [12], activation of protein kinase C [13], [14], and inhibition of nitric oxide synthesis [15].

Compounds 1 and 2 inhibited *A. suum* NFRD in the micromolar range (Table 1). However, their IC_{50} values against bovine NADH oxidase (complexes I + III + IV) were more than 10 times higher. Therefore, 1 and 2 showed selectivity against the nematode NFRD (Turkey's test; IC_{50} values between complexes I and II, p < 0.05).

Next, we evaluated inhibitory activities of 1 and 2 against each complex using submitochondrial particles (SMP) of *A. suum* and bovine heart (Table 2). Compound 1 inhibited complex I about 15 times more potently than complex II in *A. suum* (IC_{50} values between complexes I and II, p < 0.05). Its inhibitory activities against bovine heart complexes I and II, and III were very weak (IC_{50} values between *A. suum* and bovine complex I, p < 0.05). Therefore, 1 inhibits *A. suum* complex I selectively. The inhibitory activities of 2 against *A. suum* complexes I and II are similar to those of 1. Its inhibitions against bovine heart complexes I, II, and III were moderate. Therefore, 2 is a inhibitor of *A. suum* complex I, but it inhibits mammalian enzymes more potently than 1.
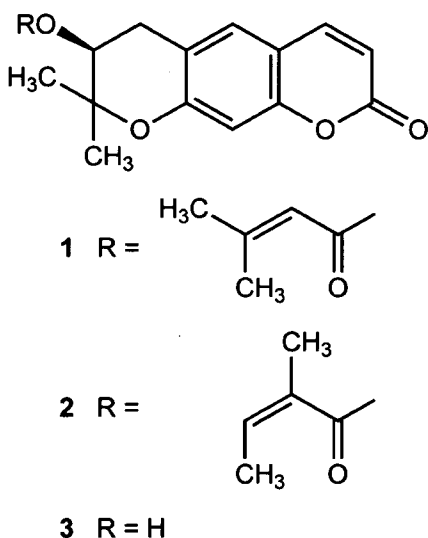

Fig. 1 Structures of decursin (1), decursinol angelate (2), and decursinol (3).

Compounds 1 and 2 are pentenoic acid esters of decursinol (3), which has been also isolated from *A. gigas* [7]. It has been reported that some biological activities of 1 and 2 were correlated with those of 3 but other activities were not correlated [11], [16], [17], [18]. Therefore, we prepared 3 from 1 and evaluated the enzyme inhibitory activities of 3. Compound 3 inhibited *A. suum* NFRD and bovine NADH oxidase at concentrations similar to 1 and 2 (Table 1). However, 3 also potently inhibited *A. suum* complex II and bovine heart complexes II and III (Table 2). Its inhibitions against *A. suum* and bovine heart complex I were both weak. It is interesting that the selective inhibition against *A. suum* complex I or II depends on whether the ester moiety exists or not. *H. pylori* is known to have NFRD [19], and 1 and 2 were reported to inhibit the growth of *H. pylori*, whereas the inhibition by 3 was weak [11]. It is suggested that the growth inhibition of *H. pylori* by 1 and 2 may be due to the selective inhibition of complex I.

It is also interesting that the inhibition of bovine complex III is affected by the side-chain ester structure. Compound 3 with no side-chain ester is the most favorable for complex III inhibition. The extension of angelic acid in 2 caused an eight-fold increase of the IC_{50} value. The isomer, senecioic acid, in 1 hampered complex III inhibition, which may be due to the steric hindrance of the methyl group. A similar tendency was also observed for the inhibition of bovine complex II.

As for the effects on electron transport enzymes, 1 and 3 were reported to inhibit chloroplast-mediated electron transport only in the dark [16]. They inhibited the photophosphorylation activities of chloroplasts, but the inhibition exhibited by 3 was more potent than that of 1. The correlation between electron transport enzymes and photophosphorylation requires further study.

Materials and Methods

NMR spectra were recorded on Varian Inova 600 or Mercury 300 spectrometers. Mass spectra were obtained on a JEOL JMS-AX505 HA spectrometer. Optical rotations were recorded on a JASCO model DIP-181 polarimeter.

The roots of *Angelica gigas* Nakai (Apiaceae) were purchased at a Korean registered market, and the quality was controlled according to the Korean Pharmacopoeia. The roots were collected in Chungcheongbuk-do, Korea, in 2002.

The dried root powder of *Angelica gigas* Nakai (200 g) was treated with 2000 mL of acetone twice. The extracts were combined, concentrated, and partitioned between EtOAc (2000 mL) and water (2000 mL). The EtOAc layer was concentrated to give 17.8 g of dark green oil. Subsequently, 1.7 g of the oil were charged on a silica gel column (63–200 μm, 4.1×12 cm, Merck KGaA; Darmstadt, Germany) and eluted stepwise with hexane-EtOAc 80:20 (500 mL), 70:30 (1000 mL), 60:40 (500 mL), and 50:50 (500 mL). Fractions of 50 mL were collected and monitored by NFRD inhibition and TLC (Merck No. 105715, hexane-EtOAc 50:50). Fraction 16 (750–800 mL), which had potent NFRD inhibitory activity and showed a single spot on silica gel TLC, was concentrated to yield 524 mg of yellow oil. Of this oil, 49.0 mg were applied to HPLC (Senshu pak Pegasil ODS,

Table 1 Inhibitory activities of NFRD and NADH oxidase by 1–3

Compound	IC_{50} (μM)	
	NFRD (A. suum)	NADH oxidase (bovine heart)
1	1.09 ± 0.03[a]	65.0 ± 7.1[a]
2	2.71 ± 1.00[b]	43.0 ± 4.5[b]
3	4.80 ± 0.63[c]	35.7 ± 9.1[c]

[a,b,c] Items with the same letters were significantly different (p < 0.05).

Table 2　Inhibitory activities of 1–3 on electron transport complexes

| Compound | A. suum SMP | | IC_{50} (µM) | bovine heart SMP | |
	complex I	complex II	complex I	complex II	complex III
1	6.42 ± 0.19[a]	112 ± 13[a]	60.1 ± 7.0[a]	>100	>100
2	8.40 ± 1.40[b]	81 ± 25[b,c,d]	45.9 ± 3.7[b]	35.2 ± 1.4[c]	17.0 ± 1.2[d]
3	>100	3.86 ± 0.73[e]	40.6 ± 5.3[e,f,g]	1.41 ± 0.20[f]	2.10 ± 0.12[g]

[a,b,c,d,e,f,g] Items with the same letters were significantly different (p < 0.05).

2×25 cm; Senshu Scientific Co.; Tokyo, Japan), elued with CH_3CN-H_2O 60:40; flow 8 mL/min, column temperature 40 °C; detection of eluates by a multiwavelength detector MD-910 (JAS-CO). The major peak (t_R = 25 min) was collected and concentrated under vacuum to give 45.8 mg of colorless oil. It was further purified by HPLC (Senshu pak Pegasil Silica, 2×25 cm, Senshu Scientific Co.); eluted with hexane-EtOAc 85:15, flow 8 mL/min, column temperature 40 °C; detection of eluates by MD-910. Two peaks were eluted at 55 min and 51 min, which were identified as 1 (13.5 mg) and 2 (9.5 mg), respectively.

Decursin (1): colorless oil; HR-FAB-MS: m/z = 329.1393 [M + H]$^+$ (calcd. for $C_{19}H_{21}O_4$: 329.1389); [α]$_D^{22}$: +144.2 (c 0.2, MeOH). The ^{1}H- and ^{13}C-NMR data were the same as those previously reported [12].

Decursinol angelate (2): colorless oil; HR-FAB-MS: m/z = 329.1393 [M + H]$^+$ (calcd. for $C_{19}H_{21}O_4$: 329.1389); [α]$_D^{22}$: +114.6 (c 0.2, MeOH). The ^{1}H- and ^{13}C-NMR data were the same as previously reported [12].

Decursinol (3) was prepared from 1 as reported previously [11]. Decursin (1, 5.0 mg) was dissolved in 0.5 mL of MeOH, and 2.0 mL of 1 M NaOH were added to the solution. After the solution had been stirred at room temperature for 75 min, its pH was adjusted to 3 by 1 M HCl and extracted with EtOAc. The organic layer was concentrated (4.0 mg) and purified by HPLC (Senshu pak Pegasil ODS, 2×25 cm); 30% CH_3CN, 8 mL/min, 40 °C; detection of eluates by MD-910. The major peak eluted at 27 min was collected to give 2.2 mg of 3.

Decursinol (3): colorless oil; HR-FAB-MS: m/z = 247.0978 [M + H]$^+$ (calcd. for $C_{14}H_{15}O_4$: 247.0970). The ^{1}H-NMR data was the same as those previously reported [20].

Enzyme assays were performed as described previously [2]. Results are expressed as the mean ± S. D. of 3 independent experiments. An analysis of variance (ANOVA) followed by Turkey's test was applied to study the enzyme inhibition selectivity.

Acknowledgements

References

1 Kita K, Nihei C, Tomitsuka E. Parasite mitochondria as drug target: diversity and dynamic changes during the life cycle. Curr Med Chem 2003; 10: 2535–48.

2 Ōmura S, Miyadera H, Ui H, Shiomi K, Yamaguchi Y, Masuma R et al. An anthelmintic compound, nafuredin, shows selective inhibition of complex I in helminth mitochondria. Proc Natl Acad Sci USA 2001; 98: 60–2.

3 Ui H, Shiomi K, Yamaguchi Y, Masuma R, Nagamitsu T, Takano D et al. Nafuredin, a novel inhibitor of NADH-fumarate reductase, produced by Aspergillus niger FT-0554. J Antibiot 2001; 54: 234–8.

4 Shiomi K, Ui H, Suzuki H, Hatano H, Nagamitsu T, Takano D et al. A γ-lactone form nafuredin, nafuredin-γ, also inhibits helminth complex I. J. Antibiot 2005; 58: 50–5.

5 Miyadera H, Shiomi K, Ui H, Yamaguchi Y, Masuma R, Tomoda H et al. Atpenins, potent and specific inhibitors of mitochondrial complex II (succinate-ubiquinone oxidoreductase). Proc Natl Acad Sci USA 2003; 100: 473–7.

6 Horsefield R, Yankovskaya V, Sexton G, Whittingham W, Shiomi K, Ōmura S et al. Structural and computational analysis of the quinone-binding site of complex II (succinate-ubiquinone oxidoreductase): a mechanism of electron transfer and proton conduction during ubiquinone reduction. J Biol Chem 2006; 281: 7309–16.

7 Hata K, Sano K. Constitution of decursin, a new coumarin isolated from the root of Angelica decursiva. Tetrahedron Lett; 1966: 1461–5

8 Ryu KS, Yook CS. Coumarins of the root of Angelica gigas. I. J Pharmaceut Soc Korea 1967; 11: 22–6.

9 Ryu KS, Hong ND, Kim NJ, Kong YY. Studies on the coumarin constituents of the root of Angelica gigas Nakai. Isolation of decursinol angelate and assay of decursinol angelate and decursin. Kor J Pharmacol 1990; 21: 64–8.

10 Okuyama T, Takata M, Nishino H, Nishino A, Takayasu J, Iwashima A. Studies on the antitumor-promoting activity of naturally-occurring substances. III. Structure of a new coumarin and antitumor-promoter activity of coumarins from Angelicae Radix. Shoyakugaku Zasshi 1990; 44: 346–8.

11 Bae EA, Han MJ, Kim NJ, Kim DH. Anti-Helicobacter pylori activity of herbal medicines. Biol Pharm Bull 1998; 21: 990–2.

12 Lee S, Lee YS, Jung SH, Shin KH, Kim BK, Kang SS. Anti-tumor activities of decursinol angelate and decursin from Angelica gigas. Arch Pharm Res 2003; 26: 727–30.

13 Ahn KS, Sim WS, Kim IH. Decursin: a cytotoxic agent and protein kinase C activator from the root of Angelica gigas. Planta Med 1996; 62: 7–9.

14 Ahn KS, Sim WS, Lee IK, Seu YB, Kim IH. Decursinol angelate. A cytotoxic and protein kinase C activating agent from the root of Angelica gigas. Planta Med 1997; 63: 360–1.

[15] Rho TC, Choi HC, Lee SW, Kim YH, Rho MC, Kim YK et al. Inhibition of nitric oxide synthesis by coumarins from *Polygonum cuspidatum* in LPS-activated RAW 264.7 cells. Saengyak Hakhoechi 2001; 32: 181 – 8.

[16] Chun HS, Lee CB. Changes of chloroplast-mediated electron transport activity and chlorophyll-protein complexes in barley seedlings by decursinol. Kor J Bot 1988; 31: 131 – 41.

[17] Lee CB, Lee MJ, Chi HJ, Kwon YM. Effects of decursin and decursinol on the germination and growth of plants. Kor J Bot 1976; 19: 7 – 13.

[18] Moon CK, Lee SC, Yun YP, Ha BJ, Yook CS. Effects of some coumarin derivatives on the bovine lens aldose reductase activity. Arch Pharm Res 1988; 11: 308 – 11.

[19] Chen M, Andersen LP, Zhai L, Kharazmi A. Characterization of the respiratory chain of *Helicobacter pylori*. FEMS Immunol Med Microbiol 1999; 24: 169 – 74.

[20] Nemoto T, Ohshima T, Shibasaki M. Enantioselective total syntheses of (+)-decursin and related natural compounds using catalytic asymmetric epoxidation of an enone. Tetrahedron 2003; 59: 6889 – 97.

Letter

1481

ELSEVIER

Relationship between reactive oxygen species and heme metabolism during the differentiation of Neuro2a cells

Noriko Shinjyo, Kiyoshi Kita *

Department of Biomedical Chemistry, Graduate School of Medicine, The University of Tokyo, 7-3-1 Hongo, Bunkyo-ku, Tokyo 113 0033, Japan

Abstract

Although neuronal cells are highly vulnerable to oxidative stress, recent studies suggest that production of reactive oxygen species (ROS) increases during and is essential for neuronal differentiation. In addition, we have previously found that heme biosynthesis is up-regulated during retinoic acid-induced differentiation of Neuro2a cells. In the current study, we showed that this up-regulation of heme biosynthesis during differentiation is ROS-dependent. Furthermore, we found that ROS-dependent induction of heme oxygenase, which degrades heme and acts as an anti-oxidant, and catalase, another anti-oxidant enzyme that contains heme as a prosthetic group, occurs during differentiation. These results suggest that heme biosynthesis following the degradation of heme protects Neuro2a cells from oxidative stress caused by ROS during differentiation.
© 2007 Elsevier Inc. All rights reserved.

Keywords: Neuron; Differentiation; ROS; Heme; Heme oxygenase; Catalase

Heme is an essential prosthetic group in many proteins and plays a regulatory role in cells [1]. Several groups have reported that heme is important in the nervous system. For example, a deficiency in heme causes neuronal cell death and the suppression of key neuronal genes [2,3]. Also, altered heme metabolism may be related to aging and Alzheimer's disease [4].

In addition, heme is a substrate of heme oxygenase (HO), which degrades heme to biliverdin, CO, and Fe^{2+}. Bilirubin, metabolite of biliverdin, is a potent radical scavenger and protects neuronal cells from oxidative stress [5]. In a previous study, we found that heme biosynthesis is up-regulated during retinoic acid (RA)-induced differentiation of Neuro2a cells [6], but we did not determine the signifi-

cance or identify the regulatory mechanism of this up-regulation.

Recent reports show that neuronal cells produce high levels of ROS [7,8]. ROS, which includes free radicals and peroxides, are generally highly reactive molecules and could cause significant damage to the neuronal cells. It is therefore expected that anti-oxidant systems are indispensable for neuronal survival. In general, cells possess several strategies to avoid damage by ROS, including ROS-degrading enzymes and low-molecular weight anti-oxidants. Two of the enzymatic systems, HO and catalase, require heme for activity.

In this study, we examined the relationship between the up-regulation of heme biosynthesis and ROS production during the differentiation of Neuro2a cells [6]. We specifically focused on the role of HO and catalase in the relationship between heme metabolism and ROS.

* Corresponding author. Fax: +81 3 5841 3444.
E-mail address: kitak@m.u-tokyo.ac.jp (K. Kita).

Materials and methods

Cell culture. Neuro2a cells were cultured as described previously [6] in Dulbecco's modified Eagle's medium (DMEM; Sigma–Aldrich, St. Louis,

MO, USA) supplemented with 10% (v/v) fetal bovine serum (FBS; Gibco BRL Life Technologies, Paisley, Scotland), 100 U/ml penicillin, 100 μg/ml streptomycin, and 292 μg/ml glutamine at 37 °C in a humidified 5% (v/v) CO_2 incubator. Differentiation was induced by treating the cells with 20 μM RA in DMEM containing 2% (v/v) FBS.

Detection of intracellular H_2O_2. Cells were seeded on coverslips (Grace Bio-Lab., Bend, OR) and incubated as described above (see Cell culture). H_2O_2 was detected using the fluorescent probe BES–H_2O_2 (Commercial name) (Wako, Nagoya Japan), which is converted to a fluorescent product by reaction with H_2O_2. The medium was replaced with fresh medium containing 10 μM BES–H_2O_2 with or without 10 mM *N*-acetyl cysteine (NAC) and incubated for 15 min at 37 °C in a humidified 5% (v/v) CO_2 incubator. Prior to observation, the BES–H_2O_2-containing medium was removed, and the cells on the coverslips were washed with phosphate-buffered saline (pH 7.4). Next pre-warmed medium (2% FBS/DMEM) without BES–H_2O_2 was added, and the fluorescence was detected using a NIKON ECLIPSE E600 fluorescence microscope with a 465- to 495-nm excitation filter, a 505-nm dichroic mirror, and a 515- to 555-nm emission filter.

Detection of peroxisomes by immunofluorescence microscopy. Peroxisomes were detected using a Select Alexa Fluor 488 Peroxisome Labeling kit (Molecular probes), which detects peroxisomal membrane protein 70 (PMP70). Cells were grown on coverslips, and peroxisome staining was performed according to the manufacturer's instructions. Fluorescence from Alexa Fluor 488 was detected using a NIKON ECLIPSE E600 fluorescence microscope as described above (see Detection of intracellular H_2O_2).

Quantitative real-time PCR. Total RNA was isolated from cells using TRIzol (Invitrogen, Carlsbad, CA, USA) according to the manufacturer's protocol. RNA was reverse-transcribed, and complementary DNAs were synthesized using an oligo (dT) primer. Real-time PCR was performed using a LC real-time PCR apparatus (Roche Diagnostics, Mannheim, Germany) and a Quantitect SYBR-Green RT-PCR Kit (Qiagen, Hilden, Germany) in a 20-μl volume containing 0.5 μM of each upstream primer (USP) and downstream primer (DSP) according to the manufacturer's instructions. The primers used were as follows: for β-actin, β-actin-USP (5′-tggaatcctgtggcatccatgaaac-3′), and β-actin-DSP (5′-taaaacgcagctcag-taacagtccg-3′); for 5-aminolevulinic acid synthase-1 (ALAS-1), ALAS-1-USP (5′-gtcaagcttctgaggc-3′), and ALAS-1-DSP (5′-cctggtcatcaactc-3′); for coproporphyrinogen oxidase (CPG oxidase, EC 1.3.3.3), CPG oxidase-USP (5′-ctccaggatccaggatc-3′), and CPG oxidase-DSP (5′-cctttggatggcg-caac-3′); for porphobilinogen deaminase (PBG deaminase, EC 2.5.1.61), PBG deaminase-USP (5′-ccgtagcagtgcatacagtg-3′), and PBG deaminase-USP (5′-ctggatggtggcctgcatag-3′); for catalase, catalase-USP (5′-ccagtgcgctgtagatg-3′) and catalase-DSP (5′-caatgttctcacacaggc-3′); for HO, HO-1-USP (5′-gacacctgaggtcaagc-3′) and HO-1-DSP (5′-ctctgacgaagtgacg-3′). The PCR was carried out as follows: initial denaturation at 95 °C for 10 min, followed by 40 cycles of denaturation for 10 s at 95 °C, elongation for 20 s (60 °C for β-actin and PBG deaminase; 52 °C for ALAS-1, and 58 °C for CPG oxidase, catalase, and HO-1), and annealing for 10 s at 72 °C. The mRNA levels were normalized according to the level of β-actin mRNA.

Measurement of catalase activity. Collected cells were suspended in potassium phosphate (50 mM) buffer (pH 7.0) containing 1 mM EDTA, homogenized, and centrifuged at 10,000*g* for 15 min at 4 °C. Catalase activities in the supernatants were measured using an Amplex Red reagent-based H_2O_2 detection system (Amplex Red Catalase Assay Kit, Molecular Probes) according to the manufacturer's instructions.

Measurement of HO activity. HO activity was measured by the bilirubin generation method [9,10]. In brief, cells were collected by centrifugation (1000*g* for 10 min at 4 °C), and the cell pellet was suspended in a buffer of 2 mM $MgCl_2$ in 100 mM potassium phosphate (pH 7.4), sonicated on ice, and centrifuged at 18,800*g* for 10 min at 4 °C. The supernatant was added to the reaction mixture (100 μl), which contained rat liver cytosol (0.5 mg/ml), hemin (20 μM), glucose-6-phosphate (2 mM), glucose-6-phosphate dehydrogenase (0.2 U), and NADPH (0.8 mM), and incubated for 1 h at 37 °C in the dark. The formed bilirubin was extracted with 300 μl of chloroform, and the change in optical density between 464

and 530 nm was measured (extinction coefficient = 40 mM^{-1} cm^{-1} for bilirubin).

Statistical analysis. Each experiment was performed three times. The data were plotted as the means ± SD. Student's *t*-test was used for comparisons. Differences were considered significant at $P < 0.01$ or 0.05 as indicated in the figure legends.

Results

ROS production during differentiation of Neuro2a cells'

Because neuronal cells may produce high levels of ROS [7,8], we examined whether Neuro2a cells produce ROS during RA-induced differentiation. In these experiments, we used the probe BES-H_2O_2 to measured the production of H_2O_2, which is a relatively stable molecule and thought to be a major form ROS [8].

We found that the fluorescence intensity produced by BES-H_2O_2 was significantly higher in RA-treated differentiating cells than in untreated control cells (Supplement 1a). The fluorescence was almost completely abolished by inclusion of the radical scavenger NAC (Supplement 1b), confirming that the observed fluorescence was ROS-dependent. The higher fluorescence levels were observed from around 6 h after the treatment with RA and continued thereafter (data not shown), indicating that ROS is produced in differentiating Neuro2a cells.

Effect of the radical scavenger NAC on the expression of heme biosynthetic enzymes in Neuro2a cells during RA-induced differentiation

Because we previously observed that heme biosynthesis is up-regulated during differentiation of Neuro2a cells [6] and because heme is essential for the activity of anti-oxidative enzymes, we postulated that the up-regulation of heme biosynthesis is related to the increase in ROS levels during differentiation. Therefore, we examined the effect of the radical scavenger NAC on heme biosynthesis.

We first measured the effect of NAC on the mRNA levels for rate-limiting enzymes, namely, ALAS-1 and CPG oxidase, which we previously found to be up-regulated in Neuro2a cells during RA-induced differentiation, and on the level of PBG deaminase, which did not change significantly during differentiation [6]. As shown in Fig. 1, the up-regulation of mRNA levels for ALAS-1 and CPG oxidase by RA was inhibited by NAC, whereas the mRNA level for PBG deaminase was not affected by RA or NAC. This result suggests that the up-regulation of heme biosynthesis during Neuro2a differentiation is ROS-dependent.

Alteration in the level of HO-1 mRNA and HO enzymatic activity during RA-induced differentiation in Neuro2a cells

HO plays an anti-oxidative role by converting heme into the anti-oxidant bilirubin. HO-1, the inducible form of HO,
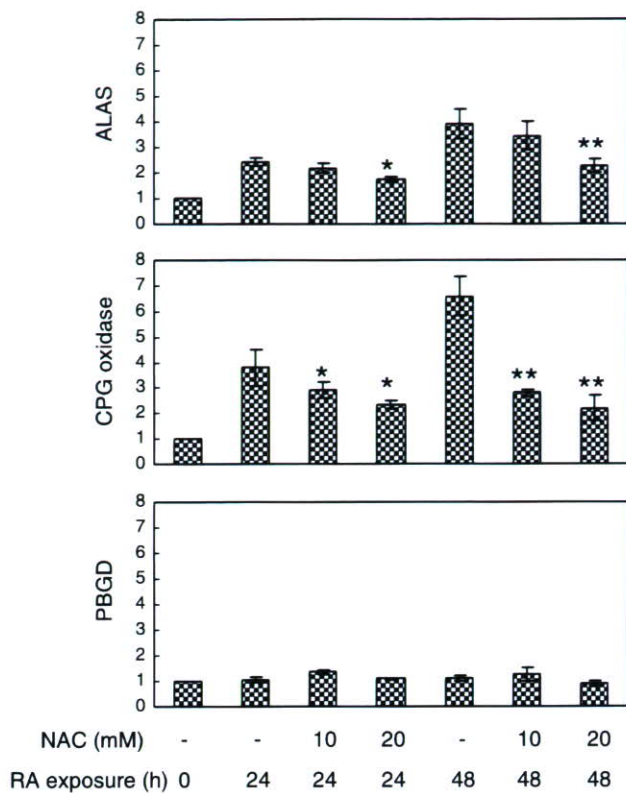
Fig. 1. Effect of NAC on the mRNA levels for heme biosynthetic enzymes. Cells were exposed to RA in the presence or absence of NAC (10 and 20 mM). The mRNA levels for heme biosynthetic enzymes ALAS-1, CPG oxidase, and PBG deaminase were measured using quantitative RT-PCR. Results represent the means ± SD ($n = 3$). $^*P < 0.05$ vs. 24 h, $^{**}P < 0.05$ vs. 48 h without NAC.

responds to various stimuli including ROS [11,12]. Because our results suggested that ROS up-regulates heme biosynthetic enzymes, we suspected that ROS increases the demand for bilirubin and therefore heme. For this reason, we examined the effect of RA on the level of HO-1 mRNA and HO enzymatic activity in Neuro2a cells.

We treated the Neuro2a cells for up to 48 h with RA, isolated total RNA, and examined the level of HO-1 mRNA by RT-PCR. As shown in Fig. 2A, the level of HO-1 mRNA increased during differentiation and was approximately 10-fold higher than in untreated control cells 12 h after the induction of differentiation with RA. The level of HO-1 mRNA did not increase thereafter. We also examined the effect of the radical scavenger NAC (10 mM) on the changes in HO-1 mRNA levels. NAC greatly suppressed the increase in HO-1 mRNA levels during differentiation (Fig. 2A). We further measured the HO enzymatic activity in Neuro2a cells exposed to RA for 12 h in the presence or absence of 10 mM NAC (Fig. 2B). HO activity increased after the induction of differentiation, and the activation of HO was greatly reduced by NAC, similar to the changes in the HO-1 mRNA level (Fig. 2A). These results show that HO is activated through the ROS-dependent induction of HO-1 during RA-induced differentiation of Neuro2a cells.

Alteration in the level of catalase in Neuro2a cells during RA-induced differentiation

Catalase is a heme-containing enzyme that catalyzes the decomposition of hydrogen peroxide (H_2O_2) to water and oxygen. Because catalase is an important anti-oxidative enzyme, we examined whether it is also induced during differentiation in Neuro2a cells.

Differentiation was induced in the presence or absence of NAC, and catalase mRNA levels were examined by RT-PCR. As shown in Fig. 2C, the expression of catalase was increased during differentiation, and this induction was suppressed by NAC. We also examined the changes in the enzymatic activity of catalase (Fig. 2D). Catalase was activated approximately 2.5-fold after 48 h of RA-induced differentiation. The activation of catalase was suppressed by NAC. These results suggested that during differentiation, like HO, catalase is activated by ROS. Compared with its effects on HO induction, NAC had a moderate effect on catalase induction. Thus, 10 mM NAC was apparently not sufficient to obtain strong inhibition, although the inhibition was more obvious at 20 mM NAC (Fig. 2D).

Effect of the heme biosynthesis inhibitor succinyl-acetone (SA) on catalase activity and peroxisomal distribution in Neuro2a cells

Because catalase contains heme as a prosthetic group, heme biosynthesis may be essential for the activation of catalase. Thus, we examined whether the inhibition of heme biosynthesis affects the activation of catalase during RA-induced differentiation. Differentiation was induced in the presence or absence of 1 mM SA, an inhibitor of heme biosynthesis, and the catalase activity was measured in cell lysates. We found that SA prevented the increase in catalase activity (Fig. 3).

Catalase is a peroxisomal protein in animal cells, and its importance in the detoxification of ROS has been described previously [13]. In addition, peroxisomes are known to be critical for the function of neurons and the nervous system [14]. Therefore, we examined whether the administration of SA affects the distribution of peroxisomes. Differentiation was induced in the presence or absence of 1 mM SA, and the peroxisomes were stained using an antibody against the peroxisomal protein PMP70. Peroxisomes were abnormally distributed in SA-treated cells. Specifically, we observed many aggregated or dot-like signals in the neurites of SA-treated cells (Supplement 2). Similar changes were also observed in cells treated with the catalase inhibitor 3-aminotriazole (3-AT) (Supplement 3).

Effect of the HO inhibitor zinc protoporphyrin IX (ZnPP IX) on the level of ALAS-1 mRNA in Neuro2a cells

As shown in Fig. 2A, the induction of HO-1 mRNA occurred in the early stage of differentiation (6–12 h) before
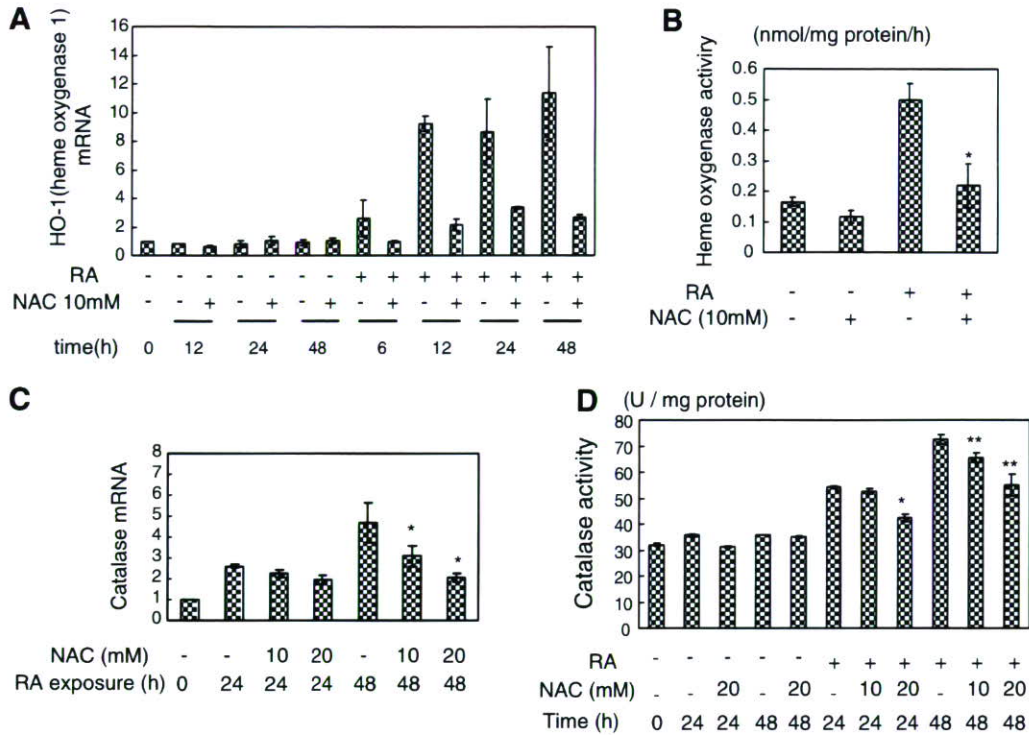
Fig. 2. (A) Changes in the level of HO-1 mRNA during RA-induced differentiation in the presence or absence of NAC. Cells were exposed to RA with or without 10 mM NAC, and HO-1 mRNA levels were measured by quantitative RT-PCR. Signals were normalized by the signal for β-actin mRNA, and the values relative to those at 0 h are presented. (B) HO activity in the presence or absence of NAC. Following a 12 h exposure to RA in the presence or absence of 10 mM NAC, cells were lysed, and HO activity was measured in the cell lysates. Results represent the means ± SD ($n = 3$). The statistical significance was evaluated using Student's t-test ($^*P < 0.01$ vs. 12 h with RA). (C) Changes in the level of catalase mRNA during differentiation in the presence or absence of NAC. Differentiation of Neuro2a cells was induced with RA in the presence or absence of NAC (10 and 20 mM). The level of mRNA for catalase was measured by quantitative RT-PCR. Results represent the means ± SD ($n = 3$). $^*P < 0.05$ vs. 24 h, $^{**}P < 0.05$ vs. 48 h without NAC. (D) Changes in catalase activity during differentiation in the presence or absence of NAC. Cell lysates were prepared, and catalase activity was measured using Amplex Red. Results represent the means ± SD ($n = 3$). $^*P < 0.01$ vs. 24 h, $^{**}P < 0.01$ vs. 48 h without NAC.
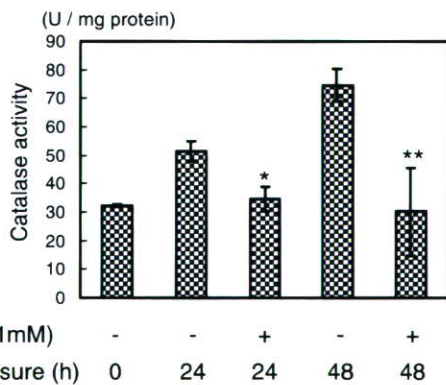

Fig. 3. Effect of SA on the changes in catalase activity. Cells were treated with RA in the presence or absence of 1 mM SA, and catalase activity was measured in cell lysates. Results represent the means ± SD ($n = 3$). $^*P < 0.01$ vs. 24 h, $^{**}P < 0.01$ vs. 48 h without SA.

the up-regulation of heme biosynthesis (∼48 h) [6], indicating that the HO-1 is a primary target of ROS. To clarify the relationship between the up-regulation of heme biosynthesis and the induction of HO activity, we examined the effect of ZnPP IX, a competitive inhibitor of HO, on the induc-

tion of ALAS-1. We found that the increase in ALAS-1 mRNA was significantly reduced by ZnPP IX (Fig. 4A), although the mRNA encoding another heme biosynthetic enzyme, CPG oxidase, was not affected by ZnPP IX (data not shown). ZnPP IX caused a significant reduction in the level of ALAS-1 mRNA at concentrations above 1 μM, which corresponded with the dose-dependence of the effects of ZnPP IX on HO activity (Fig. 4B).

Discussion

In this study, we examined the relationship between ROS and heme metabolism during the differentiation of Neuro2a cells. It has been suggested that heme plays an essential role in the differentiation of neuronal cells [2–4], but the functions of heme are diverse [15] and their significance in neuronal cells has not been fully elucidated. Based on our previous observation that heme biosynthesis is up-regulated during the differentiation of Neuro2a cells [6], our current results suggest that this is related to the activation of anti-oxidative enzymes HO and catalase.

Catalase is one of the major proteins in peroxisomes [16]. Because catalase contains heme as an essential pros-
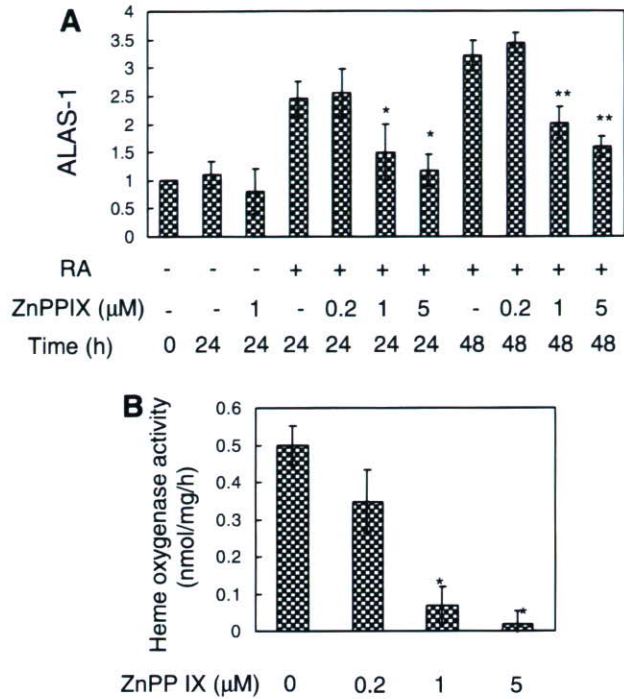
Fig. 4. (A) Effect of ZnPP IX on the level of mRNA for the heme biosynthetic enzyme ALAS-1. Cells were treated with ZnPP IX (0.2, 1, and 5 mM) and the mRNA level for ALAS-1 was measured by quantitative RT-PCR. Results represent the means ± SD ($n = 3$). *$P < 0.01$ vs. 24 h, **$P < 0.01$ vs. 48 h without ZnPP IX. (B) Effect of ZnPP IX on HO activity. Cells were exposed to RA for 12 h in the presence or absence of ZnPP IX, and HO activity was measured in cell lysates. The activity was presented as nmol bilirubin/mg protein/h. Results represent the means ± SD ($n = 3$). *$P < 0.01$ vs. without ZnPP IX.

expression was suppressed by the HO inhibitor ZnPP IX but unaffected by the catalase inhibitor 3-AT (data not shown).

In this report, we investigated the relationship between ROS and heme metabolism during RA-induced differentiation of Neuro2a cells. Previous reports have demonstrated that ROS participate in the differentiation of nonneuronal cells and that NADPH oxidase helps produce ROS [20,21]. Elevation of the level of ROS also seems to be a common phenomenon in neuronal differentiation [7,8], although the source of ROS and the signaling mechanism leading to neuronal differentiation remains to be clarified. RA is essential not only for neuronal differentiation but also for neuronal regeneration [22,23]. Therefore, the findings in this study might also be relevant to neuronal regeneration.

Acknowledgments

Appendix A. Supplementary data

Supplementary data associated with this article can be found, in the online version, at doi:10.1016/j.bbrc. 2007.04.071.

References

[1] M.A. Gilles-Gonzalez, G. Gonzalez, Heme-based sensors: defining characteristics, recent developments, and regulatory hypotheses, J. Inorg. Biochem. 99 (2005) 1–22.

[2] Y. Zhu, T. Hon, W. Ye, L. Zhang, Heme deficiency interferes with the Ras-mitogen-activated protein kinase signaling pathway and expression of a subset of neuronal genes, Cell Growth. Differ. 13 (2002) 431–439.

[3] A. Sengupta, T. Hon, L. Zhang, Heme deficiency suppresses the expression of key neuronal genes and causes neuronal cell death, Brain Res. Mol. Brain Res. 137 (2005) 23–30.

[4] H. Atamna, W.H. Frey 2nd, A role for heme in Alzheimer's disease: heme binds amyloid beta and has altered metabolism, Proc. Natl. Acad. Sci. USA 101 (2004) 11153–11158.

[5] A. Kaizaki, S. Tanaka, K. Ishige, S. Numazawa, T. Yoshida, The neuroprotective effect of heme oxygenase (HO) on oxidative stress in HO-1 siRNA-transfected HT22 cells, Brain Res. 1108 (2006) 39–44.

[6] N. Shinjyo, K. Kita, Up-regulation of heme biosynthesis during differentiation of Neuro2a cells, J. Biochem. (Tokyo) 139 (2006) 373–381.

[7] M. Tsatmali, E.C. Walcott, K.L. Crossin, Newborn neurons acquire high levels of reactive oxygen species and increased mitochondrial proteins upon differentiation from progenitors, Brain Res. 1040 (2005) 137–150.

[8] K. Suzukawa, K. Miura, J. Mitsushita, J. Resau, K. Hirose, R. Crystal, T. Kamata, Nerve growth factor-induced neuronal differentiation requires generation of Rac1-regulated reactive oxygen species, J. Biol. Chem. 275 (2000) 13175–13178.

[9] R.K. Kutty, M.D. Maines, Oxidation of heme c derivatives by purified heme oxygenase: evidence for the presence of one molecular

thetic group, our finding of simultaneous ROS-dependent up-regulation of heme biosynthesis and catalase activity suggests that heme biosynthesis plays an indispensable role in catalase activation. Thus, oxidative damage due to a deficiency in catalase activity could explain the abnormal distribution of peroxisomes observed in SA-treated cells (Fig. 3B). In fact, in the nematode *Caenorhabditis elegans* [13,17], a lack of peroxisomal catalase causes a progeric phenotype and the appearance of aggregated peroxisomes with altered morphologies [13].

Another important finding in this study was that HO-1 is induced by a ROS-dependent mechanism during differentiation. Analysis of the changes in the level of HO-1 mRNA indicated that this enzyme is induced during the very early stage of differentiation and before the induction of catalase and heme biosynthetic enzymes. HO is an anti-oxidative enzyme, and its inducible form, HO-1, is an integral part of the antioxidant system in cells [18] and is up-regulated by a variety of factors, including ROS [11,12]. It is likely that HO-1 induction is the primary target of ROS and that it contributes to the up-regulation of heme biosynthesis, possibly through the consumption of heme [19]. This may help meet demand for heme needed for catalase activation. In fact, the up-regulation of ALAS-1

species of heme oxygenase in the rat liver, J. Biol. Chem. 257 (1982) 9944–9952.

[10] J. Patel, N. Manjappa, R. Bhat, P. Mehrotra, M. Bhaskaran, P.C. Singhal, Role of oxidative stress and heme oxygenase activity in morphine-induced glomerular epithelial cell growth, Am. J. Physiol. Renal Physiol. 285 (2003) F861–F869.

[11] S.H. Chang, J. Garcia, J.A. Melendez, M.S. Kilberg, A. Agarwal, Haem oxygenase 1 gene induction by glucose deprivation is mediated by reactive oxygen species via the mitochondrial electron-transport chain, Biochem. J. 371 (2003) 877–885.

[12] J.H. Yi, A.S. Hazell, N-acetylcysteine attenuates early induction of heme oxygenase-1 following traumatic brain injury, Brain Res. 1033 (2005) 13–19.

[13] O.I. Petriv, R.A. Rachubinski, Lack of peroxisomal catalase causes a progeric phenotype in *Caenorhabditis elegans*, J. Biol. Chem. 279 (2004) 19996–20001.

[14] P.L. Faust, D. Banka, R. Siriratsivawong, V.G. Ng, T.M. Wikander, Peroxisome biogenesis disorders: the role of peroxisomes and metabolic dysfunction in developing brain, J. Inherit. Metab. Dis. 28 (2005) 369–383.

[15] A.S. Tsiftsoglou, A.I. Tsamadou, L.C. Papadopoulou, Heme as key regulator of major mammalian cellular functions: molecular, cellular, and pharmacological aspects, Pharmacol. Ther. 111 (2006) 327–345.

[16] C. Causeret, M. Bentejac, M. Bugaut, Proteins and enzymes of the peroxisomal membrane in mammals, Biol. Cell. 77 (1993) 89–104.

[17] C.S. Wood, J.I. Koepke, H. Teng, K.K. Boucher, S. Katz, P. Chang, L.J. Terlecky, I. Papanayotou, P.A. Walton, S.R. Terlecky, Hypo-catalasemic fibroblasts accumulate hydrogen peroxide and display age-associated pathologies, Traffic 7 (2006) 97–107.

[18] K. Chen, K. Gunter, M.D. Maines, Neurons overexpressing heme oxygenase-1 resist oxidative stress-mediated cell death, J. Neurochem. 75 (2000) 304–313.

[19] P.D. Drew, I.Z. Ades, Regulation of the stability of chicken embryo liver delta-aminolevulinate synthase mRNA by hemin, Biochem. Biophys. Res. Commun. 162 (1989) 102–107.

[20] J. Li, M. Stouffs, L. Serrander, B. Banfi, E. Bettiol, Y. Charnay, K. Steger, K.H. Krause, M.E. Jaconi, The NADPH oxidase NOX4 drives cardiac differentiation: Role in regulating cardiac transcription factors and MAP kinase activation, Mol. Biol. Cell. 17 (2006) 3978–3988.

[21] M. Ushio-Fukai, R.W. Alexander, Reactive oxygen species as mediators of angiogenesis signaling: role of NAD(P)H oxidase, Mol. Cell. Biochem. 264 (2004) 85–97.

[22] S. Jacobs, D.C. Lie, K.L. DeCicco, Y. Shi, L.M. DeLuca, F.H. Gage, R.M. Evans, Retinoic acid is required early during adult neurogenesis in the dentate gyrus, Proc. Natl. Acad. Sci. USA 103 (2006) 3902–3907.

[23] J. Mey, New therapeutic target for CNS injury? The role of retinoic acid signaling after nerve lesions, J. Neurobiol. 66 (2006) 757–779.

ELSEVIER

Change of subunit composition of mitochondrial complex II (succinate–ubiquinone reductase/quinol–fumarate reductase) in *Ascaris suum* during the migration in the experimental host

Fumiko Iwata [a,b], Noriko Shinjyo [a], Hisako Amino [a], Kimitoshi Sakamoto [a], M. Khyrul Islam [c], Naotoshi Tsuji [c], Kiyoshi Kita [a,*]

[a] *Department of Biomedical Chemistry, Graduate School of Medicine, The University of Tokyo, 7-3-1 Hongo, Bunkyo-ku, Tokyo 113 0033, Japan*
[b] *Department of Molecular and Cellular Physiology, Graduate School of Comprehensive Human Sciences, University of Tsukuba, Tsukuba, Japan*
[c] *Laboratory of Parasitic Diseases, National Institute of Animal Health, National Agriculture Research Organization, Tsukuba, Japan*

Abstract

The mitochondrial metabolic pathway of the parasitic nematode *Ascaris suum* changes dramatically during its life cycle, to adapt to changes in the environmental oxygen concentration. We previously showed that *A. suum* mitochondria express stage-specific isoforms of complex II (succinate–ubiquinone reductase: SQR/quinol–fumarate reductase: QFR). The flavoprotein (Fp) and small subunit of cytochrome *b* (CybS) in adult complex II differ from those of infective third stage larval (L3) complex II. However, there is no difference in the iron–sulfur cluster (Ip) or the large subunit of cytochrome *b* (CybL) between adult and L3 isoforms of complex II. In the present study, to clarify the changes that occur in the respiratory chain of *A. suum* larvae during their migration in the host, we examined enzymatic activity, quinone content and complex II subunit composition in mitochondria of lung stage L3 (LL3) *A. suum* larvae. LL3 mitochondria showed higher QFR activity (~ 160 nmol/min/mg) than mitochondria of *A. suum* at other stages (L3: ~ 80 nmol/min/mg; adult: ~ 70 nmol/min/mg). Ubiquinone content in LL3 mitochondria was more abundant than rhodoquinone (~ 1.8 nmol/mg versus ~ 0.9 nmol/mg). Interestingly, the results of two-dimensional bule-native/sodium dodecyl sulfate polyacrylamide gel electrophoresis analyses showed that LL3 mitochondria contained larval Fp (Fp^L) and adult Fp (Fp^A) at a ratio of 1:0.56, and that most LL3 CybS subunits were of the adult form ($CybS^A$). This clearly indicates that the rearrangement of complex II begins with a change in the isoform of the anchor CybS subunit, followed by a similar change in the Fp subunit.
© 2007 Elsevier Ireland Ltd. All rights reserved.

Keywords: Ascaris suum lung-stage L3 (LL3); Complex II; Quinone; NADH–fumarate reductase; Quinol–fumarate reductase (QFR); Oxidative stress

1. Introduction

During the life cycle of the parasitic nematode *Ascaris suum*, it transitions from aerobic to anaerobic metabolism in parallel with changes in the environmental oxygen concentration (Fig. 1) [1–6]. In aerobic metabolism, which is used by *A. suum* larvae during their development from fertilized egg to third stage larvae (L3), phosphoenolpyruvate (PEP) is converted to pyruvate by pyruvate kinase, and pyruvate is converted to CO_2 and H_2O via the tricarboxylic acid (TCA) cycle, generating a large amount of ATP by aerobic oxidative phosphorylation [7]. Adult *A. suum* worms, which live in a low-oxygen environment, use the anaerobic phosphoenolpyruvate carboxykinase (PEPCK)-
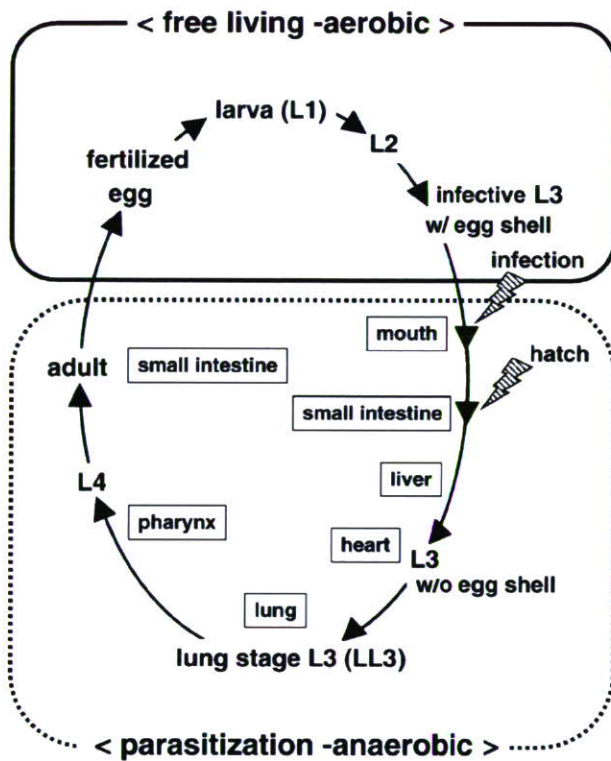
Fig. 1. Life cycle of *Ascaris suum*. Fertilized eggs grow to infective L3 under aerobic environment. Infective L3 larvae are ingested by the host, reach the small intestine and hatch there. Afterwards, larvae migrate into the host body (liver, heart, lung, pharynx), and finally migrate back to the small intestine and become adults. In the host small intestine, the oxygen concentration is only 2.5 to 5% of that of the exogenous environment [12]. w/, with; w/o, without.

succinate pathway. In the first step in the PEPCK-succinate pathway, PEPCK fixes CO_2 to PEP in the cytosol, to form oxaloacetate. This oxaloacetate is then reduced to malate, which is dismutated in mitochondria. Then, fumarate hydratase converts the malate to fumarate, which is reduced by the quinol–fumarate reductase (QFR) activity of complex II; in aerobic respiration, complex II catalyzes oxidation of succinate (succinate–ubiquinone reductase; SQR) in the mitochondria. The last step of the PEPCK-succinate pathway involves the NADH–fumarate reductase system, which is composed of complex I (NADH–quinone reductase), low-potential rhodo-quinone (RQ) and complex II (QFR) [3,8]. Electron transfer from NADH to fumarate is coupled to ATP synthesis by site I phosphorylation in complex I. The difference in redox potential between $NAD^+/NADH$ ($Em' = -320$ mV) and fumarate/succinate ($Em' = +30$ mV) is sufficient to drive ATP synthesis.

In eukaryotes, complex II is localized in the inner mitochondrial membrane, and is generally composed of 4 peptides [3]. The largest flavoprotein (Fp) subunit has an approximate molecular mass of 70 kDa and contains flavin adenine dinucleotide (FAD) as a prosthetic group. The relatively hydrophilic catalytic region of complex II is formed by the Fp subunit and the iron–sulfur cluster (Ip) subunit, whose molecular weight is about 30 kDa. The remaining subunits comprise

cytochrome *b*, which contains heme *b*. Cytochrome *b* is composed of 2 hydrophobic membrane-anchoring polypeptide subunits; the 15-kDa large subunit (CybL) and the 13-kDa small subunit (CybS). These cytochrome *b* subunits are necessary for interaction between complex II and hydrophobic membrane-associated quinones such as ubiquinone (UQ) and RQ. However, it is unclear how heme *b* is involved in the electron transfer between complex II and quinones.

In a previous study, we showed that *A. suum* mitochondria express stage-specific isoforms of complex II [5,6,9]. While there is no difference in the isoforms of the Ip and CybL subunits of complex II between L3 larvae and adult *A. suum*, they have different isoforms of the complex II subunits Fp (larval, Fp^L; adult, Fp^A) and CybS (larval, $CybS^L$; adult, $CybS^A$). Quinone species in the mitochondria also change during the life cycle of *A. suum*. In adult mitochondria, the predominant quinone is the low-potential rhodoquinone (RQ; $Em' = -63$ mV); in larvae, the predominant quinone is ubiquinone (UQ; $Em' = +110$ mV) [10]. A combination of SQR and UQ, and that of QFR and a low-potential quinone, such as RQ or menaquinone (MK), is also observed in *E. coli* and other bacteria during metabolic adaptation to changes in oxygen supply [11]. UQ has a higher potential than RQ; therefore, RQ is better suited to transferring electrons to fumarate than is UQ. In L2 and L3 *A. suum* larvae, UQ preferentially donates electrons to the cytochrome chain in the mitochondria. Thus, UQ participates in aerobic metabolism in *A. suum* larvae, whereas RQ participates in anaerobic metabolism in adult *A. suum*.

After ingestion by the definitive host, the L3 larvae penetrate the intestinal wall and reach to the lung migrating through the tissues such as liver and heart. The L3 larvae passes from lung via the trachea to the small intestine where they molt to L4 and develop into sexually maturate adult worms in the small intestine [12]. Although studies have shown a clear difference in energy metabolism between larval and adult *A. suum* mitochondria, little is known about changes in the properties of mitochondria (including respiration) during migration of *A. suum* larvae in the host.

In the present study, we examined changes in subunit composition of *A. suum* larval complex II from lung stage L3 (LL3) larvae obtained from rabbits. Enzymatic analyses showed that properties of LL3 mitochondria differed from those of L3 and adult mitochondria. Protein chemical analysis revealed that the change in complex II begins with the anchor CybS subunit, and then occurs in the Fp subunit.

2. Materials and methods

2.1. Parasites

A. suum adult worms were procured from a slaughterhouse in Tokyo, Japan. Third stage infective (L3) larvae and lung stage L3 (LL3) larvae were obtained as previously described [5,13]. All animals used in this study were acclimatized to the experimental conditions for 2 weeks before the experiment. Animal experiments were conducted in accordance with the protocols approved by the Animal Care and Use Committee, National

Institute of Animal Health (Approval nos. 589,712). For the preparation of LL3 larvae, Japanese white rabbits were made to ingest infective *A. suum* eggs (approximately 1.5×10^5 eggs per rabbit), and infected lungs were removed from the rabbits 7 days after ingestion of the eggs. The lungs were cut into 2-cm cubes using a razor blade, and the cubes were put into nylon mesh bags (KA1000, Eiken Kizai, Tokyo, Japan) in 50-ml polypropylene conical tubes filled with phosphate-buffered saline (PBS) containing 100 µg/ml penicillin and 100 µg/ml streptomycin. Those tubes were then kept in a humidified incubator at 37 °C for 4 to 5 h. During that incubation, the larvae dropped out of the bags into the bottom of the tubes. The larvae were then washed several times with fresh PBS in a 37 °C water bath. Contaminating erythrocytes from the host rabbits were eliminated by hemolysis, which was induced by washing the pellet containing LL3 larvae with pre-warmed tap water at 37 °C. The body length of the LL3 larvae, obtained from infected rabbit on day 7 post-infection, were 1.2–1.3 mm. They were slightly smaller than LL3 larvae derived from infected swine at the same post-infectious stage (1.5 mm) [14].

2.2. Preparation of mitochondria from L3, LL3 and adult A. suum

Mitochondria from L3 and adult *A. suum* muscle were prepared using the method described by Amino et al. [5]. Because that method was not applicable to LL3 mitochondria, we established the following method to obtain active mitochondria from LL3; the entire procedure was performed on ice or at 4 °C. The LL3 larvae were gently suspended in an equal volume of ice-cold suspension buffer containing 210 mM mannitol, 10 mM sucrose, 1 mM disodium EDTA and 50 mM Tris–HCl (pH 7.5), supplemented with 10 mM sodium malonate [15]. The LL3 larvae in the suspension were cut using a scalpel (No. 10 blade, Feather, Osaka, Japan) on a $90 \times 75 \times 3$-mm custom-made glass plate with a hollow (diameter, 22 mm; depth, 3 mm) in the middle. The cut larvae were then homogenized with a hand-powered glass–glass homogenizer for 15 min, and the homogenate was centrifuged at $500 \times g$ for 1 min. The resulting supernatant was centrifuged at $10,000 \times g$ for 10 min to obtain the mitochondrial pellet. The pellet was resuspended in the suspension buffer and stored at -80 °C until used. The protein concentration of the mitochondria was determined using the method of Lowry [16], using bovine serum albumin as the standard.

2.3. Enzyme assay

All assays were performed at 25 °C, using 50 mM potassium phosphate (pH 7.5) as the reaction buffer. The SQR [17], succinate dehydrogenase (SDH) [18], QFR [19] and NADH–fumarate reductase [8] activities of mitochondria were assayed as described. The NADH-decyl UQ (-dUQ) and NADH-decyl RQ (-dRQ) assays were performed using the same method as the NADH–fumarate reductase activity assay, except that 60 µM dUQ or dRQ was used as the electron acceptor, instead of sodium fumarate.

2.4. Quantitative analysis of quinone in LL3 mitochondria

Quinones were extracted from lyophilized LL3 mitochondria, and were analyzed by reverse-phase HPLC as described by Miyadera et al. [20]. The concentrations of quinones were determined spectrophotometrically using the following extinction coefficients: for UQ, $E_{1\%1\ cm}$ at 275 nm$=158$; for RQ, $E_{1\%1\ cm}$ at 283 nm$=141$ [10].

2.5. Western blotting

Complex II from L3, LL3 and adult mitochondria was analyzed by Western blotting using the method of Towbin et al. [21]. The mitochondrial proteins were separated by SDS-PAGE, using a 7.5% acrylamide gel for the Fp subunit, and using a 10/20% gradient acrylamide gel (Daiichi, Tokyo, Japan) for the Ip and CybS subunits. The proteins were then transferred to a nitrocellulose membrane at 4 °C and 80 V for 1 h. The membranes were incubated with the following antibodies in Tris-buffered saline containing 0.05% (w/v) Tween 20 (TBST) and 2% (w/v) skim milk: anti-Fp monoclonal, diluted 1:3000 [18]; anti-CybS^A monoclonal, diluted 1:5000 [5]; CybS^L peptide-based polyclonal, diluted 1:300 [5]; mixture of anti-Ip and anti-CybS polyclonal, diluted 1:2000 [5]. Each membrane was then incubated for 30 min with one of the following alkaline phosphatase-conjugated secondary antibodies: goat anti-mouse IgG (for Fp and CybS^A), or goat anti-rabbit IgG (for CybS^L, Ip and CybS). The proteins were detected using the alkaline phosphatase method. The amount of protein was normalized to the intensity of the Ip subunit at each stage, using NIH Image (a free image analyzing program for the Macintosh, developed by National Institutes of Health (NIH); www.rsb.info.nih.gov/nih-image/download.html).

2.6. Solubilization of mitochondria for blue native (BN-) PAGE

Mitochondria from L3, LL3 and adult *A. suum* (1.5 µmol/min in SDH activity) were incubated on ice for 1 h in 0.5% (w/v) sucrose monolaurate (SML) and Native PAGE^{TM} sample buffer containing 50 mM Bis–Tris, 6 N HCl, 50 mM NaCl, 10% (w/v) glycerol and 0.001% (w/v) Ponceau S in 10 mM Tris–HCl (pH 7.5) (User manual, version A 2006; www.invitrogen.com/content/sfs/manuals/nativepage_man.pdf, Invitrogen, Carlsbad, CA, USA). They were then ultracentrifuged at $200,000 \times g$ and 4 °C for 1 h, and the resulting supernatant was subjected to BN-PAGE, as described below.

2.7. BN-PAGE, CBB staining, in-gel SDH activity staining and Western blotting

The solubilized mitochondria were subjected to BN-PAGE [22] using Native PAGE Novex 4–16% Bis–Tris gels (Invitrogen). Electrophoresis was performed at 4 °C, at 150 V for 1 h, and then at 250 V, voltage constant. The cathode and anode buffers were prepared according to the user's manual of the Native PAGE Novex Bis–Tris gel system. Following the BN-PAGE, CBB staining was performed according to the user's

manual. The SDH activity of mitochondrial protein of L3, LL3 and adult *A. suum* was detected as described elsewhere [18,23]. After the BN-PAGE (first dimension), the gel cut by lane from the first-dimensional gel was equilibrated with SDS-PAGE buffer, and was then loaded onto the second-dimensional gel (7.5% acrylamide gel for Fp, and 10/20% gradient acrylamide gels (Daiichi) for Ip and CybS). The subsequent analysis by Western blotting was performed as described above.

3. Results

3.1. Enzymatic properties of LL3 complex II

Because only a small amount of LL3 larvae was obtained, and because LL3 larvae were more resistant to homogenization than L3 larvae and adult worms, we tried to establish a specific and reproducible protocol for the preparation of mitochondria from LL3 larvae. We found that cutting LL3 larvae with a scalpel was an effective method of recovering active mitochon-

dria. Using the established protocol, we obtained approximately 0.5 mg of mitochondria from 1 infected rabbit. Fig. 2 shows the results of comparative analysis of enzyme activities, relative to NADH–fumarate reductase activity, in L3, LL3 and adult mitochondria.

The Fp and Ip subunits form the hydrophilic catalytic portion of complex II, and act as a succinate dehydrogenase (SDH), catalyzing the oxidation of succinate by the water-soluble electron acceptor phenazine methosulfate. The L3 and LL3 mitochondria had almost identical levels of SDH activity, whereas the SDH activity of adult mitochondria was 2.7 to 3.9 times higher than that of L3 and LL3 mitochondria (Fig. 2A). SQR catalyzes electron transfer from succinate to the physiological electron acceptor, ubiquinone. Similarly, SQR activity of adult mitochondria was 1.8 to 3.9 times higher than that of L3 and LL3 mitochondria (Fig. 2B). QFR catalyzes a reaction that is the reverse of the reaction catalyzed by SQR. The QFR activity of LL3 mitochondria was higher than that of L3 and adult mitochondria (Fig. 2C). The NADH–fumarate
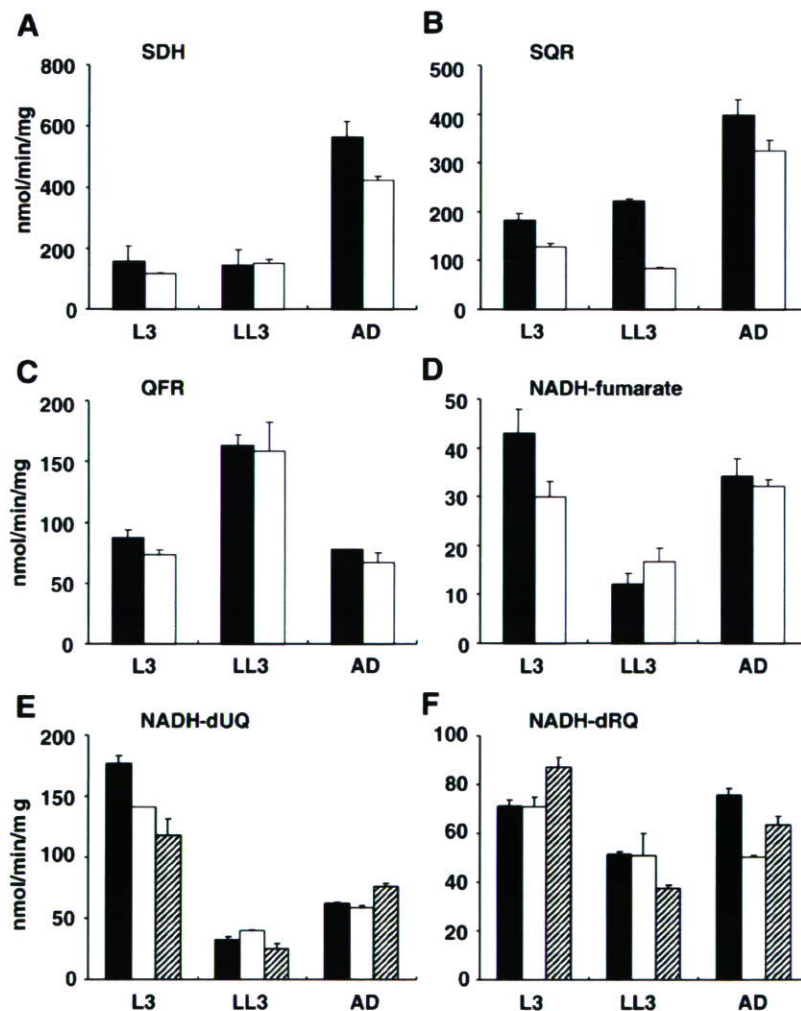
Fig. 2. Enzyme assay. Enzyme activities of complex I and II of mitochondria from L3 *A. suum* larvae, LL3 *A. suum* larvae, and *A. suum* adults. (A) SDH, (B) SQR, (C) QFR, (D) NADH–fumarate reductase, (E) NADH-dUQ and (F) NADH-dRQ. The mean and standard error were derived from triplicate measurements. Solid bars indicate experiment 1; open bars indicates experiment 2; stripe bars indicate experiment 3. Assays were performed as in materials and methods.

reductase system is an anaerobic electron-transport system of mitochondria, and is the terminal step of the PEPCK-succinate pathway. In the NADH–fumarate reductase system, the reducing equivalent of NADH is transferred to the low-potential RQ by the NADH-RQ reductase complex (Complex I). This pathway ends with the production of succinate by the rhodoquinol-fumarate reductase activity of complex II. Unexpectedly, the NADH–fumarate reductase activity of LL3 mitochondria was lower than that of L3 and adult mitochondria (Fig. 2D). The NADH-dUQ and NADH-dRQ activities of LL3 mitochondria were lower than those of L3 and adult mitochondria (Fig. 2E and F), suggesting that the low NADH–fumarate reductase activity of LL3 mitochondria is due to the lower activity of complex I in LL3 mitochondria.

3.2. Quinone components in LL3 mitochondria

Because quinone species are important low-molecular-weight mediators of electron transfer between respiratory enzymes, and because the ratio between RQ and UQ seems to be a critical factor in the direction of electron transfer in the chain, we examined the quinone content of LL3 mitochondria complex II. Although the amount of LL3 mitochondria that we obtained was quite limited, we performed the analysis using 2 different samples of LL3 mitochondria. The first sample of LL3 mitochondria contained 1.68 nmol/mg UQ-9 and 0.85 nmol/mg RQ-9. A similar result was obtained for the second sample (Table 1), indicating that the UQ content of LL3 mitochondria is approximately 2-fold greater than that of RQ. It should be noted that UQ-9 is the predominant quinone of L3 complex II (75% of the total quinone content), and that RQ is the only quinone present in complex II from adult A. suum muscle [10].

3.3. Subunit composition of the LL3 mitochondria complex II

To examine the subunit structure of complex II in LL3 mitochondria, we performed Western blotting. Because the isoforms of the Ip and CybL subunits do not change during the A. suum life cycle [5], the amount of proteins used for the Western blotting of Fp and CybS subunits was normalized to the intensity of the Ip subunit, which was visualized using the alkaline phosphatase method (Fig. 3D). LL3 mitochondrial complex II contained both Fp^L and Fp^A (Fig. 3). The LL3 and adult complex II had a Fp^L:Fp^A band intensity ratio of 1:0.56 and 1:3.5, respectively, whereas only the Fp^L band was observed in blots of L3 complex II (Fig. 3A). For the $CybS^A$ subunit, the
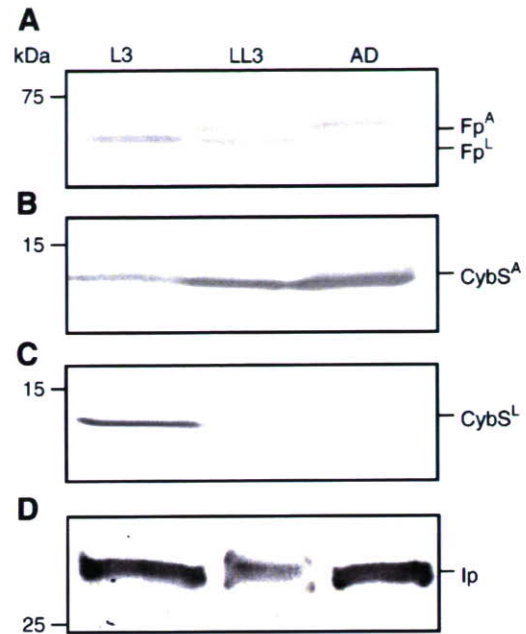

Fig. 3. Western blotting. Western blotting with (A) A. suum Fp monoclonal antibody, diluted 1:3000. (B) Monoclonal antibody against $CybS^A$ diluted 1:5000, and (C) Peptide-based polyclonal antibody against $CybS^L$ dituted 1:300. Protein levels were normalized to the Ip band intensity using (D) mixture of anti-Ip and anti-CybS polyclonal antibody diluted 1:2000. L3, A. suum larvae prepared from embryonated eggs; LL3, lung-stage L3; AD, A. suum adult. Precision Plus All Blue Standard (BIO-RAD).

L3:LL3:adult band intensity ratio was 1:3.5:6.1 (Fig. 3B). Only a small amount of $CybS^L$ was detected in LL3 mitochondria (<5% of $CybS^L$ in L3 mitochondria), and no $CybS^L$ was found in adult mitochondria (Fig. 3C). This result was reproducible in more than 3 experiments, suggesting that the subunit isoform change of LL3 complex II starts with CybS, and then occurs in Fp.

Because Western blotting clearly showed a difference in timing of isoform change between Fp and CybS subunits during migration in the host, we used BN-PAGE to examine the subunit composition of functional complex II. Mitochondrial proteins of each stage solubilized with sucrose monolaurate were subjected to BN-PAGE, and were then stained for CBB (Fig. 4A) or SDH activity (Fig. 4B) in the gel. Complex II from all 3 stages exhibited SDH activity in the gel, and band intensities of the 3 stages were almost identical when the amount of protein was normalized to 1.5 μmol/min SDH activity.

Next, we performed two-dimensional electrophoresis; with BN-PAGE as the first dimension, and SDS-PAGE as the second dimension. After the BN-PAGE, the gel was cut and was horizontally loaded onto SDS-PAGE. Following the two-dimensional electrophoresis, proteins were analyzed by Western blotting (Fig. 4C). Spots of Fps and CybSs were found in the same position as the SDH-stain band, indicating that native complex II with 4 subunits migrated during electrophoresis in the presence of the detergent. No extra spot was found in an area different from the SDH-stain position. In addition, the patterns

Table 1
Quinone quantitative analysis of LL3 mitochondria

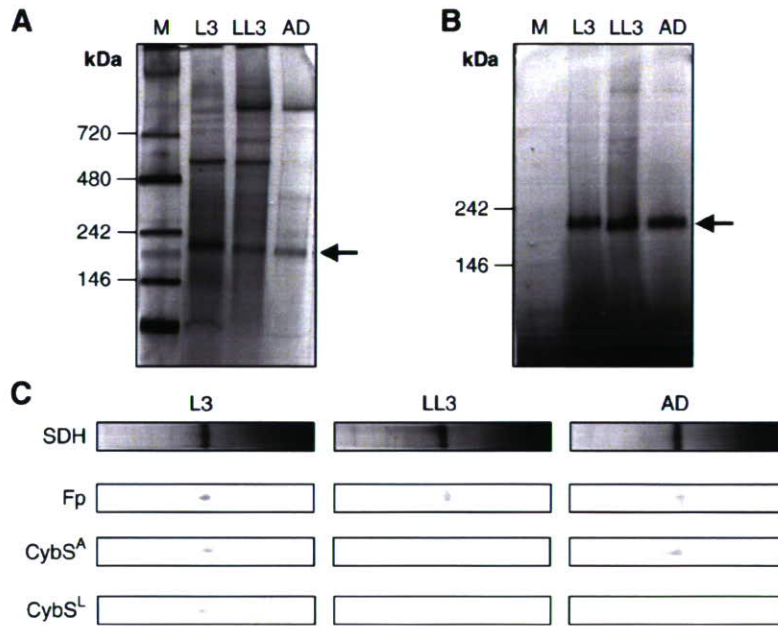| Experiment | (nmol/mg) | | Ratio |
	UQ-9[a]	RQ-9[b]	UQ-9[a]:RQ-9[b]
1	1.68	0.85	1.98:1
2	1.89	1.00	1.89:1

[a] UQ-9, ubiquinone-9.
[b] RQ-9, rhodoquinone-9.

Fig. 4. BN-PAGE analysis. BN-PAGE analysis of mitochondria from *A. suum* L3 larvae, LL3 larvae and adults (1.5 µmol/min SDH activity). (A) CBB-stain. Arrow indicates expected SDH active bands. (B) SDH activity stained in gels of Native PAGE™ Bis–Tris gel (4–16%). Arrow shows SDH active bands. (C) Western blotting after SDS-PAGE, following BN-PAGE. Antibodies used were the same as in Fig. 3. The size marker is Native Mark Unstained Protein Standard (Invitrogen).

of intensity of the spots in Fig. 4C were almost identical to the results of Western blotting after SDS-PAGE (Fig. 3).

4. Discussion

In the present study, biochemical analyses of mitochondrial complex II were performed to elucidate how complex II in *A. suum* mitochondria change its isoform composition during migration in the mammalian host. In the first step of this study, we examined complex II from LL3 larvae (Fig. 1), because there is an established method of sample collection from rabbit lung, and because several properties of LL3 have been well studied [13,24]. The natural host of *A. suum* is swine so that we need pigs for developing the migratory phase and the adult stages. However, pig rearing facilities are currently quite limited for the purpose of doing *Ascaris* infection. Helminth researchers have previously examined the life cycle and worm burdens in rabbits [25,26]. The results showed that several criteria such as the organ migratory routes and recovery of larvae in rabbits were quite similar to those in pigs, indicating that rabbit can be fairly used for permissive hosts. Actually, *Ascaris* researchers including our group have employed rabbits to do biochemical experiments of the roundworms [27,28].

We previously demonstrated that *A. suum* mitochondria express stage-specific isoforms of complex II; i.e., the flavoprotein subunit (Fp) and the small subunit of cytochrome *b* (CybS) of complex II isolated from L3 infective eggs differ from those of adult muscle complex II, while the 2 forms of complex II have an identical iron-sulfur cluster subunit (Ip) and large subunit of cytochrome *b* (CybL). Therefore, the subunit isoform composition of complex II must change during

migration in the host. To our surprise, Western blot analyses showed that both the Fp^L and Fp^A isoforms (in the ratio of 1: 0.56) were present in LL3 mitochondria, while the majority of CybS subunit was of the isoform $CybS^A$ (Fig. 3A and B). This means that expression of adult Fp does not synchronize with that expression of adult CybS, and suggests that LL3 complex II has a different combination of subunit isoforms than L3 and adult complex II.

To analyze the native state of complex II subunit composition in LL3 mitochondria, we used BN-/SDS-PAGE two-dimensional electrophoresis (Fig. 4C). The spots of the subunits were found at the same position as the SDH bands,

Table 2
Enzyme activities of L3, LL3 and adult complex I and II of *Ascaris suum* mitochondria

Assay	Experiment	Specific activity (nmol/min/mg)		
		L3	LL3	Adult
SDH	1	158±36	145±16	566±15
(complex II)	2	118±5.6	152±25	424±22
SQR	1	184±28	224±8.3	400±63
(complex II)	2	129±16	84.1±4.0	326±43
QFR	1	87.8±6.0	164±8.6	78.5±0.058
(complex II)	2	73.5±7.6	159±47	66.8±16
NADH–fumarate	1	43.0±10	12.3±4.4	34.4±7.1
reductase (complex I,II)	2	30.1±6.4	16.7±5.6	32.3±2.6
NADH-dUQ	1	177±12	32.3±5.6	62.4±1.9
	2	141±0.92	39.8±1.9	58.6±4.6
(complex I)	3	118±26	24.8±8.8	76.3±4.9
NADH-dRQ	1	71.4±4.4	51.6±2.0	75.7±5.6
	2	71.0±7.8	51.0±18	50.3±1.3
(complex I)	3	87.1±8.5	37.6±2.4	63.4±7.6

without any extra spots. This result indicates that the spots detected were derived from active complex II consisting of 4 subunits. In LL3 mitochondria, all 4 larva-/adult-types of Fp-CybS subunits was observed, while Fp^L, CybS^A and CybS^L subunit isoforms were detected in L3 mitochondria, and Fp^L, Fp^A and CybS^A subunit isoforms were detected in adult mitochondria. The pattern of the intensity of the spots in Fig. 4C is consistent with that of the Western blotting after SDS-PAGE (Fig. 3), indicating that mitochondrial complex II subunit switching first occurs in CybS, and then occurs in Fp, during migration in the host.

Of the 4 possible Fp-CybS subunit combinations (Fp^L-CybS^A, Fp^A-CybS^A, Fp^L-CybS^L and Fp^A-CybS^L), Fp^L-CybS^A is the predominant combination in LL3 mitochondria. Western blot analysis of young adult mitochondria obtained from the muscle of 12-cm-long female worms showed that CybS^L had completely disappeared, whereas Fp^L remained at a ratio of Fp^L:Fp^A = 1:1.5 (data not shown), although only 1 SDH band was observed in BN-PAGE. This finding may be due to similar properties between the 2 complexes with different combinations.

However, several questions remain unanswered. Because of limited sample amount, it is difficult to purify complex II from LL3 mitochondria. Reports indicate that adult *A. suum* uses the NADH–fumarate reductase system in its anaerobic host environment; in the NADH–fumarate reductase system, the QFR activity of mitochondrial complex II plays a significant role [3,29,30]. However, we previously found that L3 complex II had higher QFR activity than adult complex II, and presumed that this was due to pre-adaptation to the dramatic change in oxygen availability during infection of the host [5]. In the present study, we found that the QFR activity of LL3 complex II was twice as high as that of L3 complex II (Fig. 2C, Table 2). The host lung is a relatively aerobic environment (13.2% O_2) [31], suggesting that the larvae pre-adapt before they migrate into the anaerobic environment of the host small intestine (5% O_2).

Although LL3 mitochondria showed the highest QFR activity of the 3 stages we examined, their NADH–fumarate reductase activity was unexpectedly low (Fig. 2D). This appears to be due to the effects of low complex I activity, as indicated by the NADH-dUQ and NADH-dRQ assays (Fig. 2E and F). The NADH–fumarate reductase system is composed of complex I (initial dehydrogenase of NADH), RQ (electron mediator), and complex II (terminal oxidase for fumarate reduction). We also examined the quinone content of the mitochondria. Analysis of the quinone contents of mitochondria isolated from unembryonated eggs, L3 larvae and adult muscle showed that the predominant quinone in larval mitochondria (which possess an aerobic respiratory chain) was UQ-9 (75% of the total quinone content) [10]. In contrast, the only quinone present in anaerobic mitochondria from adult muscle is RQ-9. Consistent with these findings, reconstitution studies using bovine heart complex I and adult *A. suum* QFR show that RQ is essential for the function of the NADH–fumarate reductase system [32]. Specifically, when RQ-9 was incorporated into the system, the maximum activity of reconstituted NADH–fumarate reductase activity was 430 nmol/min/mg of *A. suum* complex

II, while no activity was observed in the presence of UQ-9. In addition, our previous findings suggest that although *A. suum* adult complex I uses both RQ and UQ as electron acceptors, the 2 quinones have different ways of binding reaction and reaction with *A. suum* complex I [33]. It should be noted that in the present study, UQ accounted for 66% of the total quinone of LL3 complex II, which is an intermediate between those of L3 and adult complex II [10]. Further analysis of the effect of endogenous quinones in the mitochondria of the enzyme activities of complex I and complex II is needed to elucidate the unique properties of the NADH–fumarate reductase system of *A. suum*.

In the present study, we examined how mitochondrial complex II of *A. suum* changes its subunit composition, especially during migration in the host. We found that the small subunit of cytochrome *b* (CybS) starts to change its isoform before the flavoprotein (Fp) subunit does so. Further clarification of this process will require analysis of larvae from other migration stages in the host. In each stage, the metabolic pathway of *A. suum* may continue to change according to the environmental changes, even in the host body. To elucidate this dynamic change in the mitochondrial respiratory system of *A. suum* during migration, we plan to establish an experimental system using swine, which is a definitive host of *A. suum*. With such a system, further biochemical analysis should reveal novel properties of complex II in LL3 mitochondria.

Acknowledgements

References

[1] Komuniecki R, Komuniecki PR. Aerobic–anaerobic transitions in energy metabolism during the development of the parasitic nematode *Ascaris suum*. In: Boothroyd JC, Komuniecki R, editors. Molecular approaches to parasitology. New York: Wiley-Liss; 1995.

[2] Tielens AGM, Rotte C, van Hellemond JJ, Martin W. Mitochondria as we don't know them. Trends Biochem Sci 2002;27:56–72.

[3] Kita K, Takamiya S. Electron-transfer complexes in *Ascaris* mitochondria. Adv Parasitol 2002;51:95–131.

[4] Kita K. Electron-transfer complexes in *Ascaris suum*. Parasitol Today 1992;8:155–9.

[5] Amino H, Osanai A, Miyadera H, Shinjyo N, Tomitsuka E, Taka H, et al. Isolation and characterization of the stage-specific cytochrome *b* small subunit (CybS) of *Ascaris suum* complex II from the aerobic respiratory chain of larval mitochondria. Mol Biochem Parasitol 2003;128: 175–86.

[6] Amino H, Wang H, Hirawake H, Saruta F, Mizuchi D, Mineki R, et al. Stage-specific isoforms of *Ascaris suum* complex II: the fumarate reductase of the parasitic adult and the succinate dehydrogenase of free-living larvae share a common iron–sulfur subunit. Mol Biochem Parasitol 2000;106: 63–76.

[7] Kita K, Hirawake H, Miyadera H, Amino H, Takeo S. Role of complex II in anaerobic respiration of the parasite mitochondria from *Ascaris suum* and *Plasmodium falciparm*. Biochim Biophys Acta 2002;1553: 123–39.

[8] Omura S, Miyadera H, Ui H, Shiomi K, Yamaguchi Y, Masuma R, et al. An anthelmintic compound, nafredin, shows selective inhibition of

complex I in helminth mitochondria. Proc Natl Acad Sci U S A 2001;98: 60–2.

[9] Saruta F, Kuramochi T, Nakamura K, Takamiya S, Yu Y, Aoki T, et al. Stage-specific isoforms of complex II (succinate–ubiquinone oxidoreductase) in mitochondria from the parasitic nematode, Ascaris suum. J Biol Chem 1995;270:928–32.

[10] Takamiya S, Kita K, Wang H, Weinstein PP, Hiraishi A, Oya H, et al. Developmental changes in the respiratory chain of Ascaris mitochondria. Biochim Biophys Acta 1993;1141:65–74.

[11] Cole ST, Condon C, Lemire BD, Weiner JH. Molecular biology, biochemistry and bioenergetics of fumarate reductase, a complex membrane-bound iron-sulfur flavoenzyme of Escherichia coli. Biochim Biophys Acta 1985;811: 381–403.

[12] Heinz M. Encyclopedic reference of parasitology. 2nd ed. Berlin: Springer; 2001.

[13] Islam MK, Miyoshi T, Yamada M, Alim MA, Huang X, Motobu M, et al. Effect of piperazine (diethylenediamine) on the moulying proteome express and pyrophosphate activity of Ascaris suum lung-stage larvae. Acta Trop 2006;99:208–17.

[14] Miyazaki I. Helminthic zoonoses. Tokyo: International Medical Foundation of Japan; 1991. p. 295–305.

[15] Takamiya S, Furushima R, Oya H. Electron transfer complexes of Ascaris suum muscle mitochondria I. Characterization of NADH-cytochrome c reductase (complex I–III), with special reference to cytochrome localization. Mol Biochem Parasitol 1984;13: 121–34.

[16] Lowry OH, Rosebrough NJ, Farr AL, Randall RJ. Protein measurement with the folin phenol reagent. J Biol Chem 1951;193:265–75.

[17] Miyadera H, Shiomi K, Ui H, Yamaguchi Y, Masuma R, Tomoda H, et al. Atopenins, potent and specific inhibitors of mitochondrial complex II (succinate–ubiquinone oxidoreductase). Proc Natl Acad Sci U S A 2003;100: 473–7.

[18] Tomitsuka E, Goto Y, Taniwaki M, Kita K. Direct evidence for expression of Type II flavoprotein subunit in human complex II (succinate–ubiquinone reductase). Biochem Biophys Res Commun 2003;311: 774–9.

[19] Kita K, Vibat CR, Meinhardt S, Guest JR, Gennis RB. One-step purification from Escherichia coli of complex II (succinate:ubiquinone oxidoreductase) associated with succinate-reducible cytochrome b_{556}. J Biol Chem 1989;264:2672–7.

[20] Miyadera H, Amino H, Hiraishi A, Taka H, Murayama K, Miyoshi H, et al. Altered quinone biosynthesis in the long-lived clk-1 mutants of Caenohabditis elegans. J Biol Chem 2001;276:7713–6.

[21] Towbin H, Staehelin T, Gorton J. Electrophoretic transfer of proteins from polyacrylamide gels to nitrocellulose sheets: procedure and some applications. Proc Natl Acad Sci U S A 1979;76: 4350–4.

[22] Shägger H, Cramer WA, von Jagow G. Analysis of molecular mass and oligomeric states of protein complexes by blue native electrophoresis and isolation of membrane protein complexes by two-dimensional native electrophoresis. Anal Biochem 1994;217:220–30.

[23] Kho CW, Park SG, Lee DH, Cho S, Oh GT, Kang S, et al. Activity staining of glutathione peroxidase after two-dimensional gel electrophoresis. Mol Cell 2004;18:369–73.

[24] Geenen PL, Bresciani J, Boes J, Pedersen A, Eriksen L, Fagerholm HP, et al. The morphogenesis of Ascaris suum to the infective third-stage larvae within the egg. J Parasitol 1999;85:616–22.

[25] Jeska EL, Williams JF, Cox DF. Ascaris suum: larval returns in rabbits, Guinea pigs and mice after low-dose exposure to eggs. Exp Parasitol 1969;26: 187–92.

[26] Stormberg BE, Soulsby EJL. Ascaris suum: immunization with soluble antigens in the Guinea pig. Int J Parasitol 1977;7:287–91.

[27] Komuniecki PR, Vanover L. Biochemical changes during the aerobic–anaerobic transition in Ascaris suum larvae. Mol Biochem Parasitol 1987;22(2–3):241–8.

[28] Islam MK, Miyoshi T, Kasuga-Aoki H, Isobe T, Arakawa Y, Matsumoto Y, et al. Inorganic pyrophosphatase in the roundworm Ascaris and its role in the development and molting process of the larval stage parasites. Eur J Biochem 2003;270: 2814–26.

[29] Kita K, Shiomi K, Omura S. Advances in drug discovery and biochemical studies. Trends Parasitol 2007;23:223–9.

[30] Kuramochi T, Hirawake H, Kojima S, Takamiya S, Furushima R, Aoki T, et al. Sequence comparison between the flavoprotein subunit of the fumarate reductase (complex II) of the anaerobic parasitic nematode, Ascaris suum and the succinate dehydrogenase of the aerobic, free-living nematode, Caenorhabditis elegans. Mol Biochem Parasitol 1994;68: 177–87.

[31] Martini FH, Ober WC, Garrison CW, Welch K, Hutching RT. Fundamentals of anatomy and physiology. 4th ed. Upper Saddle River, New Jergy: Prentice Hall; 1998.

[32] Kita K, Takamiya S, Furushima R, Ma YC, Suzuki H, Ozawa T, et al. Electron-transfer complexes of Ascaris suum muscle mitochondria. III. Composition and fumarate reductase activity of complex II. Biochim Biophys Acta 1998;935: 130–40.

[33] Yamashita T, Ino T, Miyoshi H, Sakamoto K, Osanai A, Nakamaru-Ogiso E, et al. Rhodoquinone reaction site of mitochondrial complex I, in parasitic helminth, Ascaris suum. Biochim Biophys Acta 2004;1608: 97–103.